Development of Forecast Information Requirements and Assessment of Current Forecast Skill Supporting the Preliminary Viability Assessment of FIRO on Lake Mendocino

Dave Reynolds[1], Scott Sellars[1], F. Martin Ralph[1], Julie Kalansky[1]

[1]*Center for Western Weather and Water Extremes (CW3E), Scripps Institution of Oceanography (UCSD)*

Based on research supported by the U.S. Army Corps of Engineers, Sonoma County Water Agency and California's Department of Water Resources (Principle Investigator: F.M. Ralph)

13 December 2016

Executive Summary

The FIRO Workplan (FIRO Steering Committee, 2015) laid out the need to identify and quantify what types of meteorological and hydrologic forecasts would be needed to enable FIRO on Lake Mendocino, to assess recent skill in the associated predictions, and to develop new forecast skill parameters as needed. On the hydrological side, the analysis focused on identifying how long it would take to release water and for it to travel downstream past flood prone areas. On the meteorological side, this analysis focuses heavily on atmospheric river (AR) conditions, which are the primary cause of extreme precipitation and flooding on the Russian River.

The FIRO Workplan called for a preliminary viability assessment (PVA) of the potential for FIRO, followed by a full viability assessment (FVA). Completion of the PVA is targeted for early 2017 and the FVA in 2020. It also laid out a research agenda that serves both the near-term needs of the PVA specifically and anticipates needs for new information to support the FVA. This report summarizes results from several analyses, including identifying forecast lead time requirements, assessing past and current forecast skill and identifying the leading causes of forecast errors. These include both traditional hydrometeorological variables such as precipitation and streamflow, and emerging needs for information on the characteristics of atmospheric rivers at landfall, as well as soil moisture conditions.

Detailed analyses of requirements have been established for both forecast lead times and what constitutes extreme rainfall for the Lake Mendocino watershed during this first year of research. Lead times of 4-7 days were established by determining the travel time of water releseases from Coyote Valley Dam (CVD) to downstream vunerable locations such as Guerneville assuming various background flow rates. Extreme rainfall rates were established utilizing both the current Water Contral Manual and establishing rainfall rates that generate high flows (>2500 cfs day^{-1}) at Ukiah and thus >8,000 cfs at Hopland, that can compromise release volumes of CVD. The rates that are critical to CVD operations are =>0.5"6hr^{-1}, => 1"

$24h^{-1}$ taken from the WCM, and =>2" $24h^{-1}$, which was found to be closely related to high flows at Ukiah and Hopland and high inflows to Lake Mendocino of > 2500 cfs day^{-1}. These high flows could restrict releases from COY dam and are thus significant to monitor.

To establish the current skill, verification analysis was completed on the CNRFC 6-hr, 24-hr and 3-day and 5-day total rainfall forecasts utilizing the 2000-2016 forecast database. Utilizing probablity of detection (POD), false alarm rates (FAR) and critical success index (CSI) skill scores (for which a value above 0.5 indicates the forecasts is correct more often than it is wrong) show that reliable forecasts for these thresholds are from 2.5 to 4 days. It was also found that the 3 and 5-day total rainfall forecasts have the same accuracy as the day 1 24-hr rainfall forecasts, with R^2 values of near 0.8 The trend in forecasting the more extreme rainfall totals, such as 3"/3days or 5"/5days, shows the CNRFC bias has trended to near zero from what was a low bias of more than 1 inch back in the early 2000's. This would indicate that there is fair confidence in utilizing a 5-day inflow QPF forecast to indicate potential runoff but less confidence in getting the peak inflow right given this is strongly a function of the 6-hr rain rates. Thus, future efforts should be placed on improving the models ability to better forecast the timing and intensity of AR landfalls which will improve the 6-hr forecasts that are critical for obtaining accurate timing and intensities of peak inflows. Further, the skill in forecasting no significant rainfall (> 1"/24hr) is very high out through 5 days with the worst forecast error from a five day forecast. This was an under-prediction of 3 inches leading to an inflow error of 2500 cfs or ~5000 ac-ft. This is a significant finding with regard to increased water storage potential under FIRO. The Global Ensemble Forecast System (GEFS) 24-hr mean rainfall, used by the CNRFC Hydrologic Ensemble Forecast System, which is used by the SCWA Ensemble Forecast Operations (EFO) Model, has less skill compared to the CNRFC deterministic 24-hr rainfall through day 5. This suggest the 61 member ensemble used by the SCWA tool should be generated using the 5-day determininstic forecast for first 5 days and the GEFS mean from days 6-15.

Inflow forecasts to Lake Mendocino utilizing the CNRFC 2005-2016 database were also verified. The same skill scores were computed for the 90th, 95th, and 99th% inflow volumes. The 90th percentile value for both 24-hour and 72-hour volumes show good CSI values (> .5) for all forecast periods out to 5-days lead time. The 95th percentile value for 24-hour volumes shows good skill out to forecast day 3, before the CSI value drops below 0.5 for forecast lead day 4 and 5. The 95th percentile value for 72-hour volumes show good CSI values for forecast lead time day 1 and 2. The 99th percentile value for 24-hour volume skill decreases rapidly past day 1, whereas the 72-hour volumes maintain CSI values above 0.4 for both day 1 and 2 forecast lead times.

In the Russian River basin contributions from the top 10% of wet days explain 81% of variance in the fluctuations of total water-year precipitation. ARs are responsible for most of the 10% wettest days. The upslope vapor transport summed over the duration of an AR landfall has a very high correlation (r^2=0.62) with total rainfall at a downwind coastal mountain site. Forecast challenges with ARs are the timing, location, and duration and intensity of the ARs at landfall, and the impact of mesoscale frontal waves (MFW) that can occur along the AR that can either disrupt the precipitation once heavy rain begins or stall the heaviest precipitation over a given area. Two events demonstrate the impacts of MFW's on AR precipitation. A tool has been developed and improved based on the GEFS forecast probability of weak to moderate ARs making landfall along the Pacific Coast. It also indicates the duration of these conditions. It provides the forecaster/decision maker with the risk of extreme rainfall occurring over the next 16 days.

1.0 Introduction

The Center for Western Weather and Water Extremes (CW^{3}E) was established in 2013 within the Scripps Institute of Oceanography. Its mission is to provide 21st Century water cycle science, technology, and outreach to support effective policies and practices that address the impacts of extreme weather and water events on the environment, people, and the economy of Western North America . Included in this report are key findings of CW^{3}E's research efforts during year one of its 5- year contract with the U.S. Army Corp. of Engineers (USACE), Engineering Research and Development Center (ERDC). As part of this first year effort CW^{3}E set out to address several of the key and immmediate research needs to support the Preliminary Viability Assessment as outlined in Table 1.1 taken from the Lake Mendocino Forecast Informed Reservoir Operations (FIRO) workplan Table 8.1. This report will address several of these key research activities, specifically those items in bold type. In addition to these, several key forecasts requirements will be quantified utilizing observations of historical events within the watershed to address where future improvements need to be focused.

Table 1.1 Immediately required research activities

Forecasting/Prediction Improvements & Tools
Quantify past performance of weather and streamflow predictions, and reservoir operations
Improve the detecting and tracking of ARs over the Pacific Ocean and at landfall
Determine the causes of major forecast errors in past strong ARs and flood events
Improve forecasting of AR landfall position, strength and orientation
Improve prediction of the duration of AR conditions over the Russian River Watershed
Diagnose the role of mesoscale frontal waves in causing long-duration AR conditions over the Russian River Watershed
Study the origins and predictions of the strong high pressure ridge that persisted over the Eastern Pacific in recent winters
Develop a specialized weather prediction model tailored to AR and precipitation prediction for the Russian River Watershed
Develop reforecasting data set to improve bias-correcting and post-processing of precipitation forecasts
Improve exceedance/non-exceedance extreme precipitation forecasts from 0-10 days lead times
Test the value of assimilation of measurements using dropsondes released from aircraft offshore
Improving microphysics in numerical weather models to improve forecasts of orographic precipitation
Quantify aerosol impacts on orographic precipitation in the region
Implement an enhanced hydrometeorological monitoring network

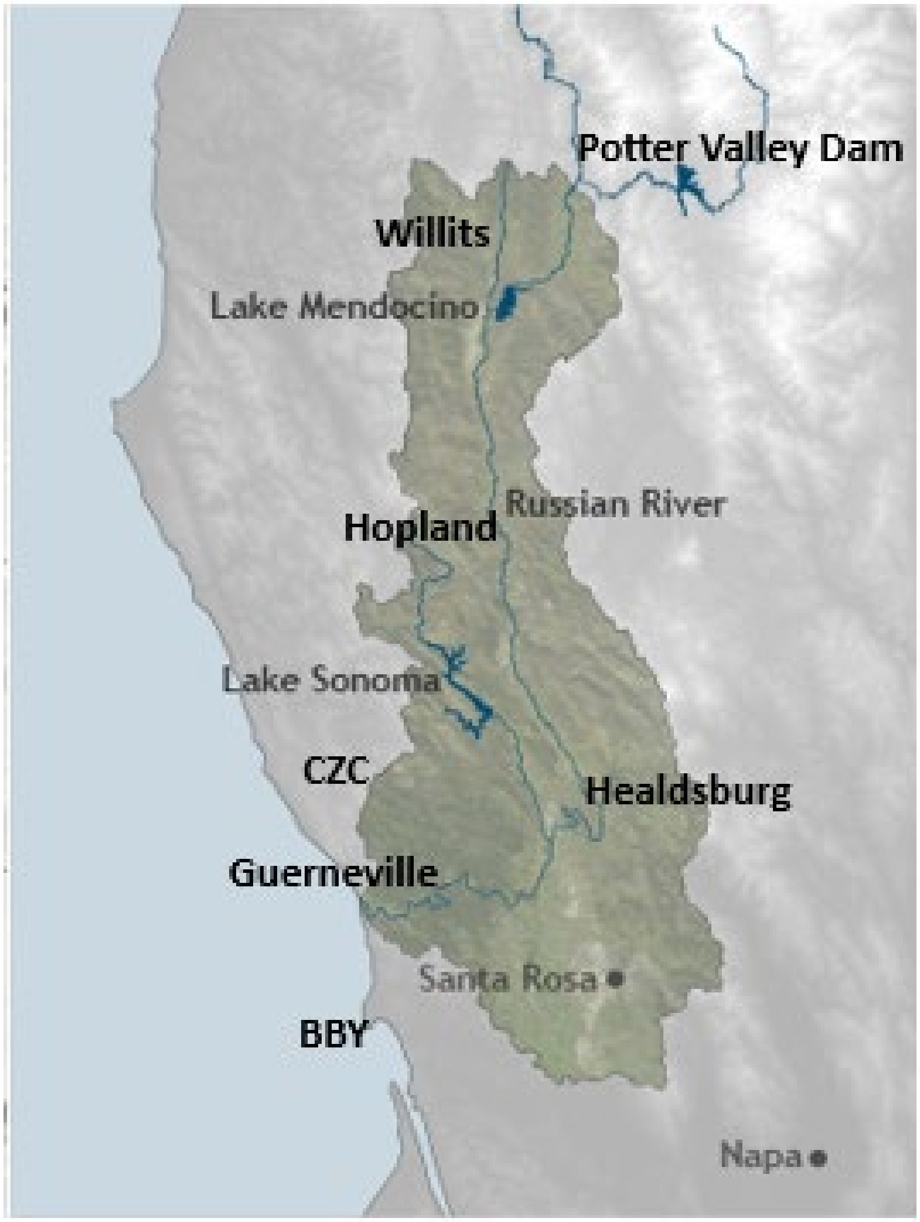

Figure 1.1 Russian River basin highlighted with locations referenced in this summary report.

2.0 Determining Travel Time of Releases from Coyote Valley Dam to Downstream Locations: Setting Forecast Lead-Time Requirements - Preliminary Results

2.1 Introduction

The Coyote Valley Dam (CVD) Water Control Manual (WCM) defines certain criteria that control the releases from CVD, during flood operations. These criteria may restrict outflows during high water downstream of CVD, especially as observed at the United States Geological stream gage near Hopland (Station Number 11462500). -When flows are at or above 8,000 cfs at the Hopland gage, releases from CVD cannot exceed the minimum of 25 cfs. Because of this restriction, under a FIRO scenario, pre-releases of water from the reservoir would be desirable if the reservoir is expected to reach critical levels (spillway elevations when an extreme rainfall event such as an atmospheric river (AR) is expected. To minimize downstream impacts from possible high releases from CVD, it is necessary to understand the travel time of the release pulse downstream. Thus, this study attempts to quantify travel times from CVD to Guerneville under various release rates to emulate possible minimum and maximum travel times and thus what forecast lead-times would be necessary to insure there is no increase in flood risk to downstream locations from pre-releases.

2.2 Analysis

Using a Lag and K model provided by SCWA, we performed two synthetic studies on travel times of Lake Mendocino release flows based on lag time parameters provided by the California Nevada River Forecast Center (CNRFC). The Lag and K model is a simple hydrologic routing method and can be used to estimate the travel time of reservoir release wave as it propagates downstream. One important note is that the Lag and K model is a simplistic realization of streamflow routing with the assumption that no local additional runoff is included (e.g., tributary runoff). A general validation study by SCWA of the models using historical low-flow data shows the Lag and K models for different case studies can capture the release wave propagation down the Russian River adequately (not shown).

This synthetic study is a general assessment of travel time for the basin as far down as Guerneville using the Lag and K model. The two synthetic scenarios analyzed a low flow release case (releases during low flows downstream) and a medium flow release case (based on the 90th percentile cool seasonal (December to April) flow for the four major control points). Both cases use the ramping rates developed by NMFS and USACE issued on April 16, 2016 to release 4938 AF over 40 hours.

Results are summarized in Figures 2.1 and 2.2, and general conclusions include proposed FIRO release strategies, which, given the various scenarios, will range between 31-92 hours (from the time when the release from CVD is initiated, to the time where the release wave is no longer impacting Guerneville). Although the release wave can be seen impacting the local flows between this range, the peak flow timing of the release wave is important for any potential FIRO-based operational release decisions.

The peak flow from the release wave moving downstream impact Guerneville at 32 hours (low flows downstream) and 31 hours (high flows downstream). Given the discussions with USACE, it is suggested that this is a time frame the operators can handle and have enough operating flexibility to be able to initiate a FIRO release strategy. It should be noted that Lake Mendocino releases only account for ~7% of the flow downstream due to its size relative to the entire Russian Basin. This is important because the FIRO operating range will be dependent on the operating scenario, including storm type, forecast and flow rates downstream. For both scenarios investigated here, we set the release to 4938 AF from the dam, which takes a total of 40 hours to complete. Tables 1 and 2 show the peak flow impact at four major control points downstream, Hopland, Cloverdale, Healdsburg Guerneville.

2.3 Conclusions

General conclusions suggest that releasing 4938 af-ft over 40 hours (including the ramp up and ramp down time) could have an impact on the peak of the downstream hydrographs for the selected locations from 31 to 32 hours after the release begins. One observation is that the peak flow timing impact downstream is a function of: (1) the time that the release is at its maximum flow rate and (2) flow conditions downstream. Further research will quantify this relationship for determining optimal releases, dependent on conditions and storage and consider additional travel time modeling approaches to capture more dynamic circumstances. Additional research will include quantifying these results and focus on uncertainty quantification of release, dependent on multiple criteria including ramping rates, downstream flow conditions and storage proposed to release. From these preliminary results, it was concluded that an approximate 4 to 7-day lead time would be needed to release approximately 5000AF and for that release to be out of the system before the heavy rains from an AR and its associated runoff commences, although the impacts of the peak flow of the release wave have impacts less than 4-days. This is conceptualized in Figure 2.3.

Location	Peak Flow (cfs)	Lag time (hours after release)
Hopland, CA	2500	20
Cloverdale, CA	2466	21
Healdsburg, CA	2258	25
Guerneville, CA	1920	32

Table 2.1. Low Flow Synthetic Case Study: Peak flows and reservoir release impact lag time (in hours) for four major control points downstream from Lake Mendocino, Hopland, Cloverdale, Healdsburg and Guerneville, CA.

Location	Peak Flow (cfs)	Lag time (hours after release)
Hopland, CA	2972	20
Cloverdale, CA	3151	21
Healdsburg, CA	3497	24
Guerneville, CA	3869	31

Table 2.2. Medium Flow Synthetic Case Study: Peak flows and reservoir release impact lag time (in hours) for four major control points downstream from Lake Mendocino, Hopland, Cloverdale, Healdsburg and Guerneville, CA.

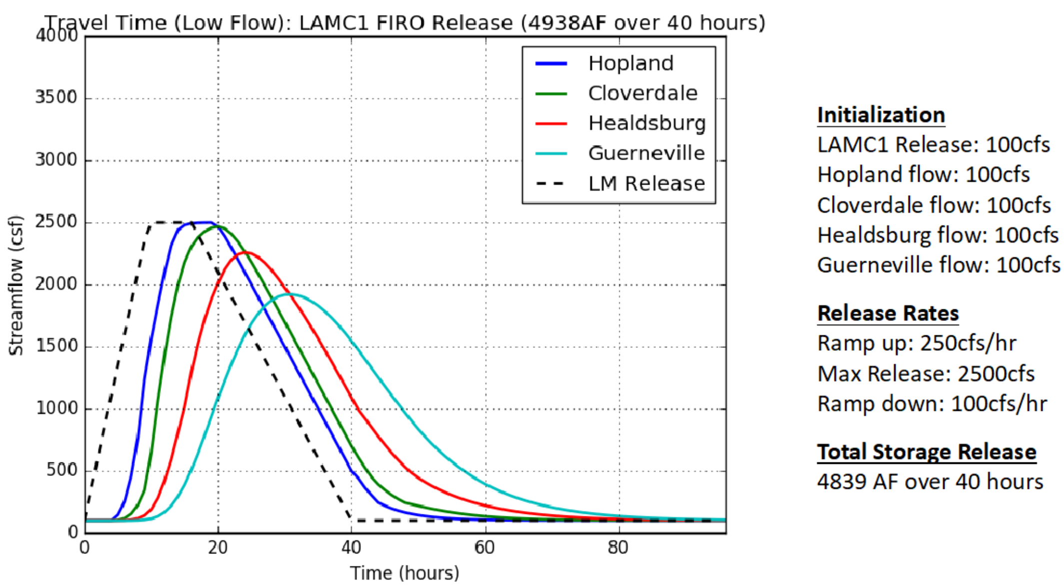

Figure 2.1. The synthetic low flow scenario where the downstream flows are low with a goal of releasing 4938 ac-ft is shown. Dashed line represents the release rates (flow in cfs) from Lake Mendocino. Blue, Green and Purple lines represent the hydrograph response to the release at Hopland, Cloverdale and Healdsburg, CA, respectively.

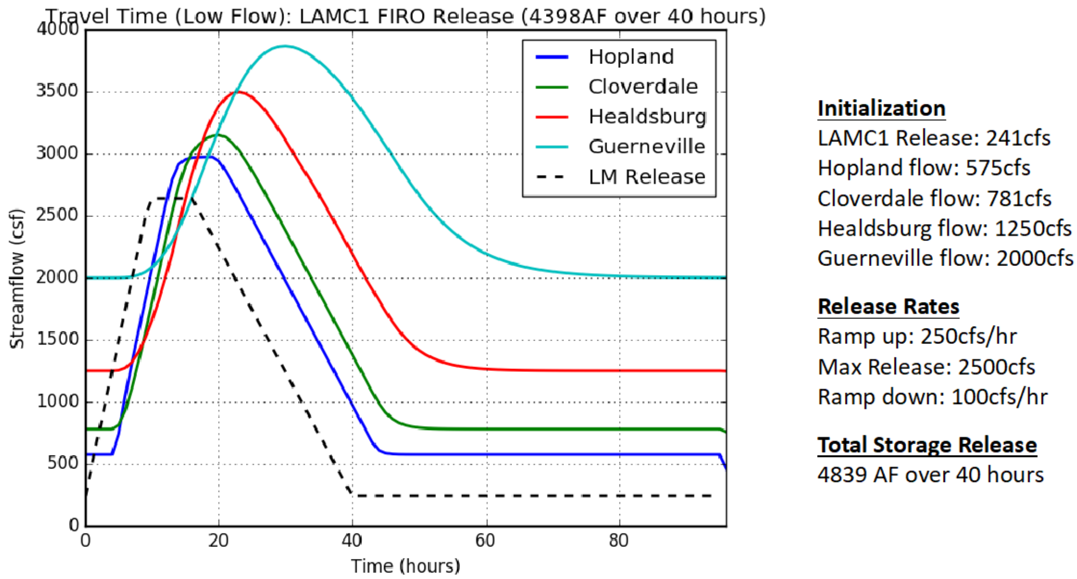

Figure 2.2 The synthetic medium flow scenario, where the downstream flows were selected from observed flows, with realistic medium range flows with a goal of releasing 4938 ac-ft is shown. Dashed line represents the release rates (flow in cfs) from Lake Mendocino. Blue, Green and Purple lines represent the hydrograph response to the release at Hopland, Cloverdale and Healdsburg, CA, respectively.

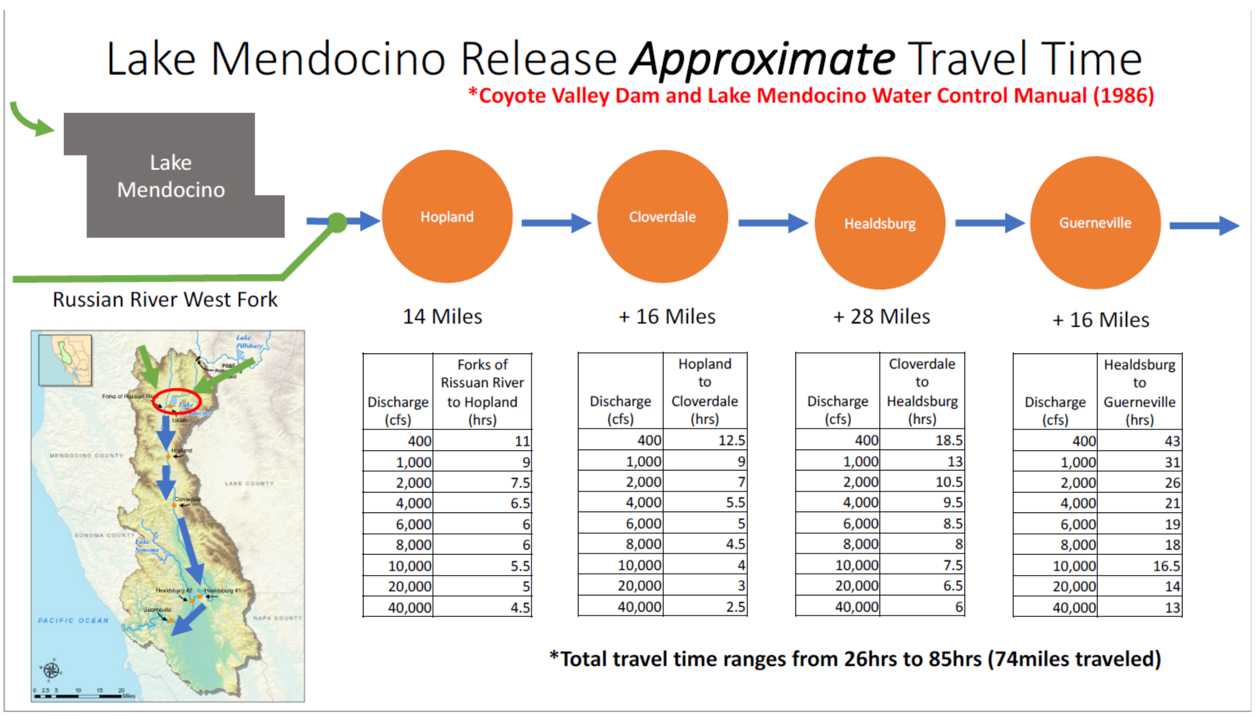

Discharge (cfs)	Forks of Rissuan River to Hopland (hrs)
400	11
1,000	9
2,000	7.5
4,000	6.5
6,000	6
8,000	6
10,000	5.5
20,000	5
40,000	4.5

Discharge (cfs)	Hopland to Cloverdale (hrs)
400	12.5
1,000	9
2,000	7
4,000	5.5
6,000	5
8,000	4.5
10,000	4
20,000	3
40,000	2.5

Discharge (cfs)	Cloverdale to Healdsburg (hrs)
400	18.5
1,000	13
2,000	10.5
4,000	9.5
6,000	8.5
8,000	8
10,000	7.5
20,000	6.5
40,000	6

Discharge (cfs)	Healdsburg to Guerneville (hrs)
400	43
1,000	31
2,000	26
4,000	21
6,000	19
8,000	18
10,000	16.5
20,000	14
40,000	13

Figure 2.3. Conceptual graphic of the forecast lead time required to pre-release a volume of 10,000 ac-ft and have it pass out of harm's way prior to a significant AR landfall. Given the approximate travel times shown there is at a minimum at 4-7 day lead time requirement for forecasting AR landfall. .

3.0 Defining Extreme Precipitation Thresholds Impacting Operations of Coyote Valley Dam (CVD): Establishing Requirements for Extreme Rainfall Events

3.1 Introduction

The current CVD WCM lists several criteria with regard to rainfall rates in the Lake Mendocino watershed that alert the dam operator to potential significant runoff flowing into the reservoir. The two listed rainfall rates are 0.5"/6hrs and 1"/24hrs. These rainfall rates were used to verify the CNRFC's 6-hr and 24-hr day 1-5 forecast of mean areal precipitation (MAP) as described in Section 4. In addition, the WCM states *"Flood control releases from Lake Mendocino are also guided by downstream maximum flow criteria defined in the WCM. When flow at the USGS Russian River near Ukiah gage (West Fork gage) exceeds 2,500 cfs and is rising, Russian River flows at the USGS Russian River near Hopland gage (Hopland gage) are monitored hourly to assess for any needed release reductions. The WCM requires that controlled flood releases cannot contribute to flows greater than 8,000 cfs at Hopland gage. When flows at the Hopland gage exceed 8,000 cfs due to unimpaired flows downstream of CVD, reservoir releases cannot exceed the minimum release requirement of 25 cfs*. To summarize, the flows on the West Fork gage reaching 2,500 cfs and rising are a proxy for flows at Hopland reaching 8,000 cfs. The flows on the West Fork are highly correlated to the inflows to Lake Mendocino. Thus determining the rainfall above Lake Mendocino that produces 2500 cfs inflows will also be a proxy for flows at Hopland reaching 8,000 cfs. As noted when flows reach this level at Hopland releases from CVD are reduced to 25 cfs. There are several reasons for this, including the desire not to exacerbate downstream high water and flows given channel capacity limitations and issues with high flows causing downstream turbidity and impacts on fisheries. These factors place additional restrictions on how fast water can be evacuated once the reservoir elevation encroaches into the flood pool. CW3E sought to address the question:

What is the rainfall over the upper Russian watershed over a 24-hr period that can lead to daily flows at or above an average of 2500 cfs/day at Ukiah and Lake Mendocino (and thus 8,000 cfs at Hopland) that would then potentially restrict reservoir releases?

3.2 Analysis

Observed daily full natural inflows to Lake Mendocino of 2500 cfs or greater were compared to the corresponding daily Lake Mendocino watershed MAP. This is shown in Figure 3.1 for period 1978-2010. The mean MAP was computed to be 2.02”/day. Figure 3.1 removed days with runoff above 2500 cfs following heavy rain events but with little additional precipitation falling. A second method utilized daily rainfall at Willits Howard Ranger Station, a key gauge used by the CNRFC in the QPF predictions and just upstream in the headwaters of the West Fork of the Russian of which the Ukiah stream gage is used to measure runoff. Figure 3.2 shows the results of this analysis utilizing the period from 1986 to 2016. These results also indicate that the average rainfall producing 2500 cfs daily flows or greater at Ukiah is over 2 inches (2.7 inches). It was noted that for this past 2015-2016 winter the correlation between flows at the Ukiah stream gage and inflows to Lake Mendocino had a correlation of 0.97. Only one day had flows at Ukiah above 2500 cfs (2630 cfs) and inflows to Lake Mendocino below 2500 cfs (2400 cfs).

3.3 Conclusions

It is important to establish the requirements of the forecast system that would be used in the FIRO decision support system (to be developed). This analysis shows that the forecast of 2”/24 hrs in the upper Russian Basin can lead to flows at Hopland approaching 8,000 cfs. This in turn will impact releases from CVD both as too how much should be released prior to heavy rainfall and what can be released during heavy rainfall. With this in mind, the next section evaluates the current skill in forecasting the three critical rainfall-rates of .5”/6hrs, 1”/24hrs and 2”/24hrs.

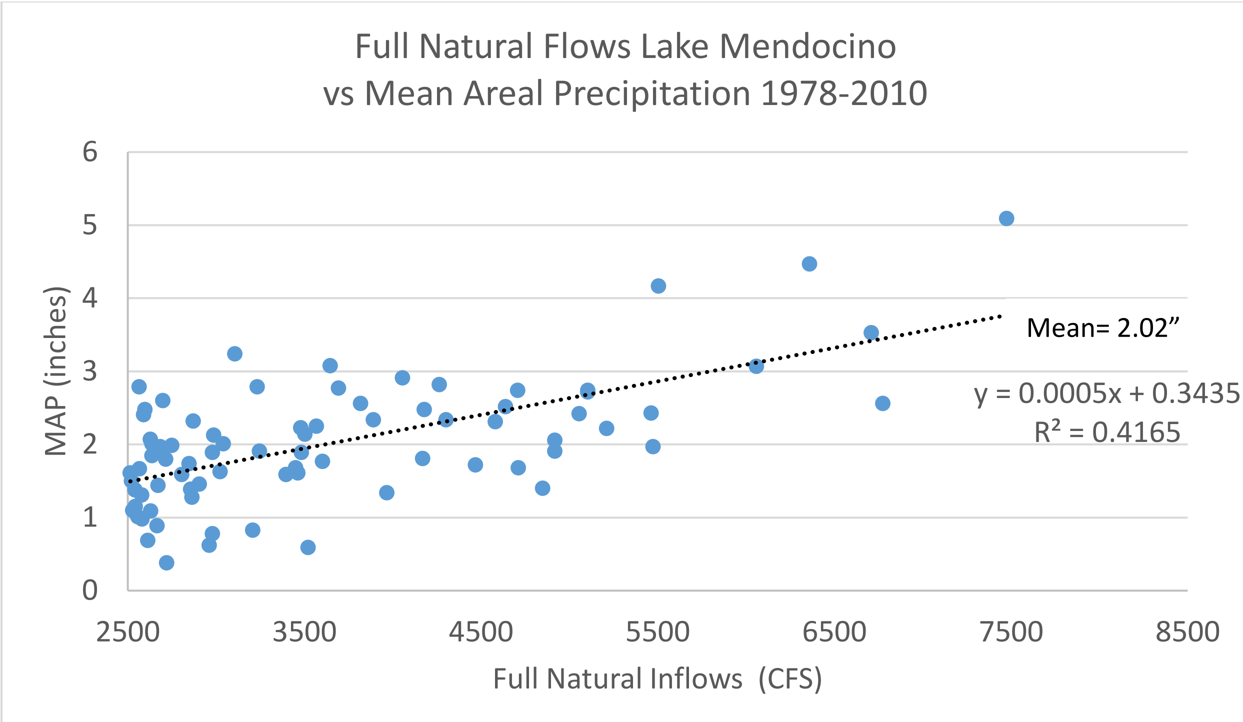

Figure 3.1 Scatter plot of mean areal precipitation for the Lake Mendocino watershed and daily average full natural inflows to Lake Mendocino at or greater than 2500 cfs for period 1978 to 2010. Mean daily MAP was calculated at 2.02 in/day.

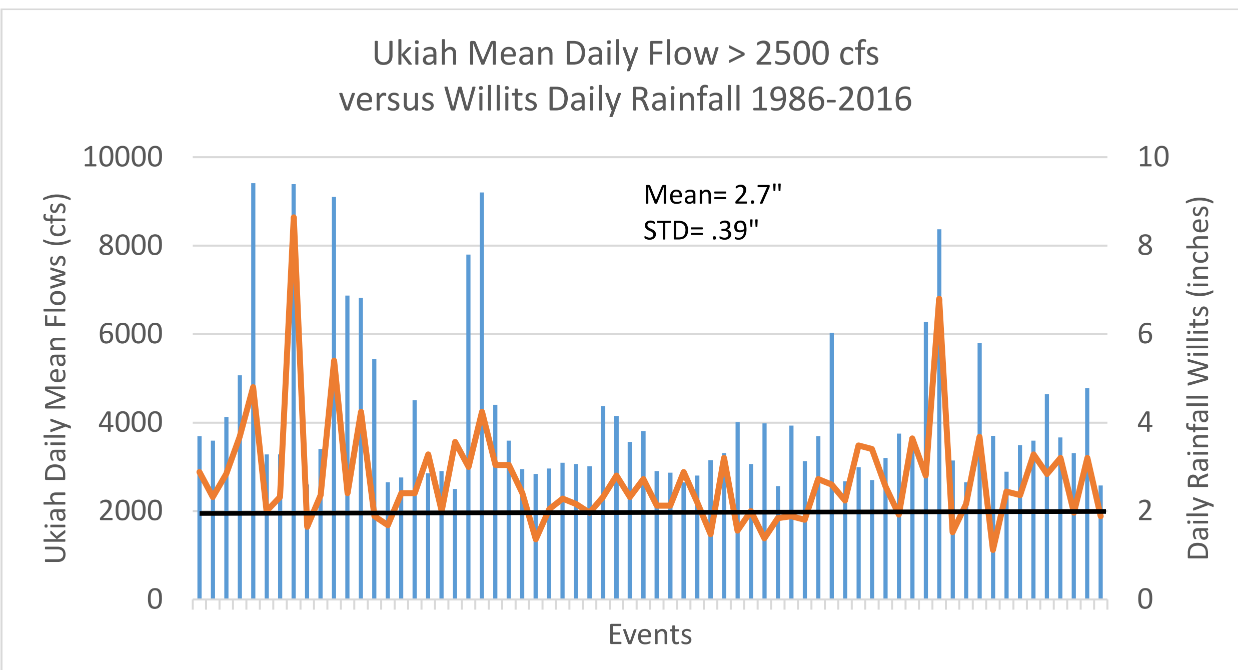

Figure 3.2 Graph shows daily average flows at Ukiah on the West Fork Russian at or above 2500 cfs (blue bars) and daily rainfall totals at Willits Howard Ranger Station (orange line) located in the headwaters of the West Fork watershed.

4.0 Current Forecast Skill Levels for Rainfall Impacting Coyote Valley Dam Operations: CNRFC QPF Verification Results

4.1 Introduction

The FIRO Work Plan Table 8.1 (shown earlier), identified a pressing research need to define past forecast skill in quantitative precipitation forecasts (QPFs) that are the basis for making streamflow forecasts. It has already been identified that there are three critical rain rates that have a direct impact on CVD operations and thus would impact a future FIRO decision system. To meet this research need, historical CNRFC QPFs were analyzed to determine the current accuracy and skill levels to define a baseline for future comparisons and quantify improvements.

4.2 Analysis

The CNRFC issues 6-hr MAP forecasts for the Lake Mendocino watershed daily beginning at 1200 UTC and extending out 5 days. These 6-hr forecasts are directly input to the Community Hydrologic Prediction System (CHPS) to forecast inflows to Lake Mendocino that are used by the USACE to determine possible increases in releases if the reservoir is encroached or expected to encroach into the flood pool. Thus, it is useful to determine the accuracy of the QPF forecasts that feed CHPS and how this accuracy declines with forecast lead time.

To conduct this study, CW^3E worked closely with the CNRFC, which provided daily individual 6-hr 5-day forecasts along with the observed Lake Mendocino MAPs for the period from January 2000 through April of 2016. Each 6-hr forecast was paired with the 6-hr observed MAP for the entire period of record to determine both the Coefficient of Determination (square of correlation coefficient or R^2) and the root mean square error (RMSE).

Figure 4.1 shows the R^2 values and RMSE for these 6-hr QPFs utilizing the 2000-2016 dataset. As expected, the forecast accuracy systematically falls-off with forecast lead time. Using the QPF as a predictor, it explains only 20% of the variance in observed MAP at day 5 which indicates low predictive accuracy. Summing the 6-hr MAPs into 24, 72 and 120-hour totals tends to reduce forecast errors by eliminating timing errors of the Numerical Weather Prediction (NWP) model guidance used to prepare the forecasts (Demargne et al., 2014). Figure 4.2 shows the 24-hr values along with the 3-day and 5-day total MAP forecast values. Note that the 3 and 5-day R^2 values are comparable to the day 1 24-hr QPF. This is important in that the 3-and 5-day runoff volume can be as important for reservoir operations as the timing and magnitude of the peak inflow; the operator can be more confident that if a large volume of runoff is indicated over the next 3-5 days and the reservoir is encroached into the flood pool, pre-releases ahead of this flow may be necessary under FIRO as flows at Hopland may restrict releases during the heaviest rainfall. Because reservoir storage for water supply is important, the operator does not want to release water that may not be replenished by subsequent runoff.

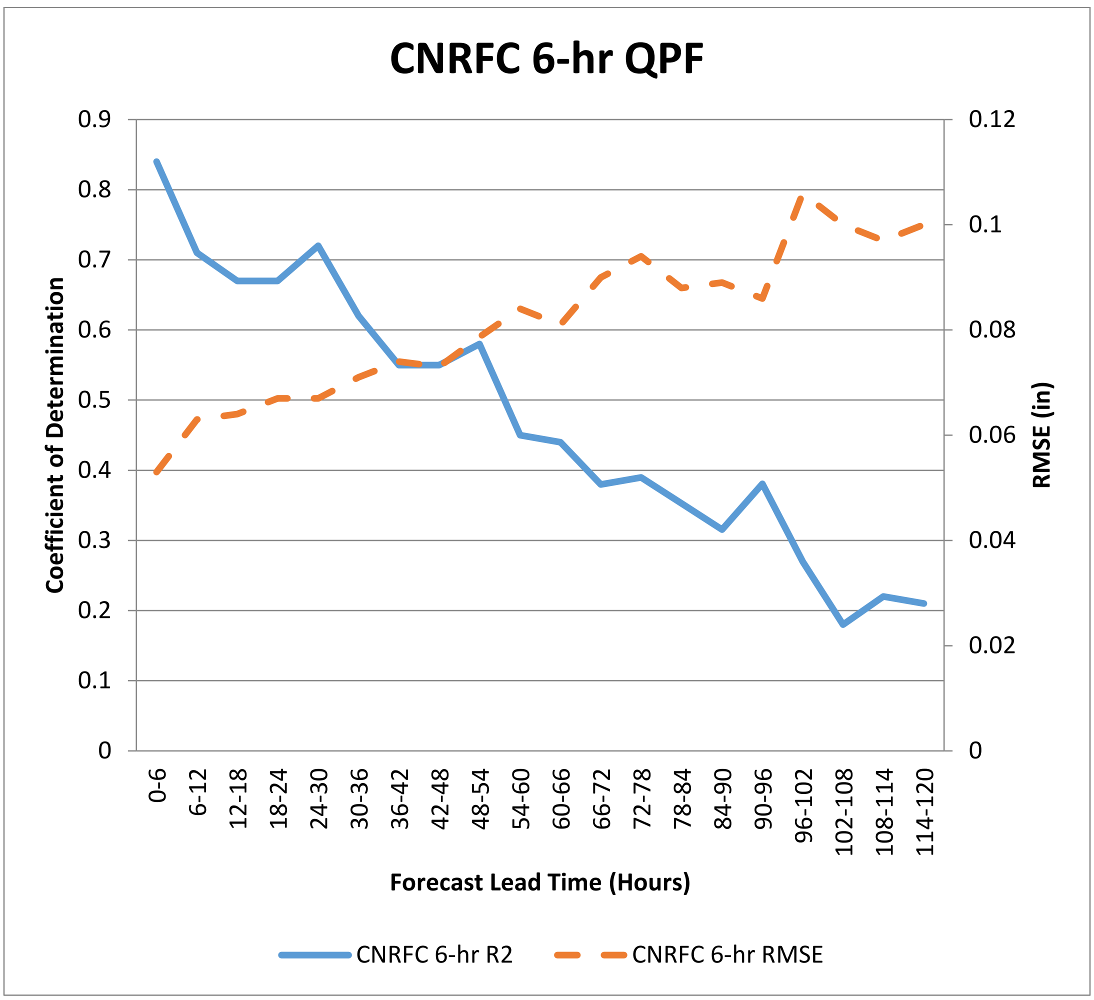

Figure 4.1 CNRFC accuracy for 6-hr QPF versus forecast lead time for period of record shows high R^2 values out through 48 hours where the QPF explains more than 50 % of the variance in observed MAPs. Using the CNRFC 6-hr QPF as a prediction of 6-hr MAPs after this time is much more unreliable. RMSE's however remain at or below .1 inches throughout the duration of the forecasts.

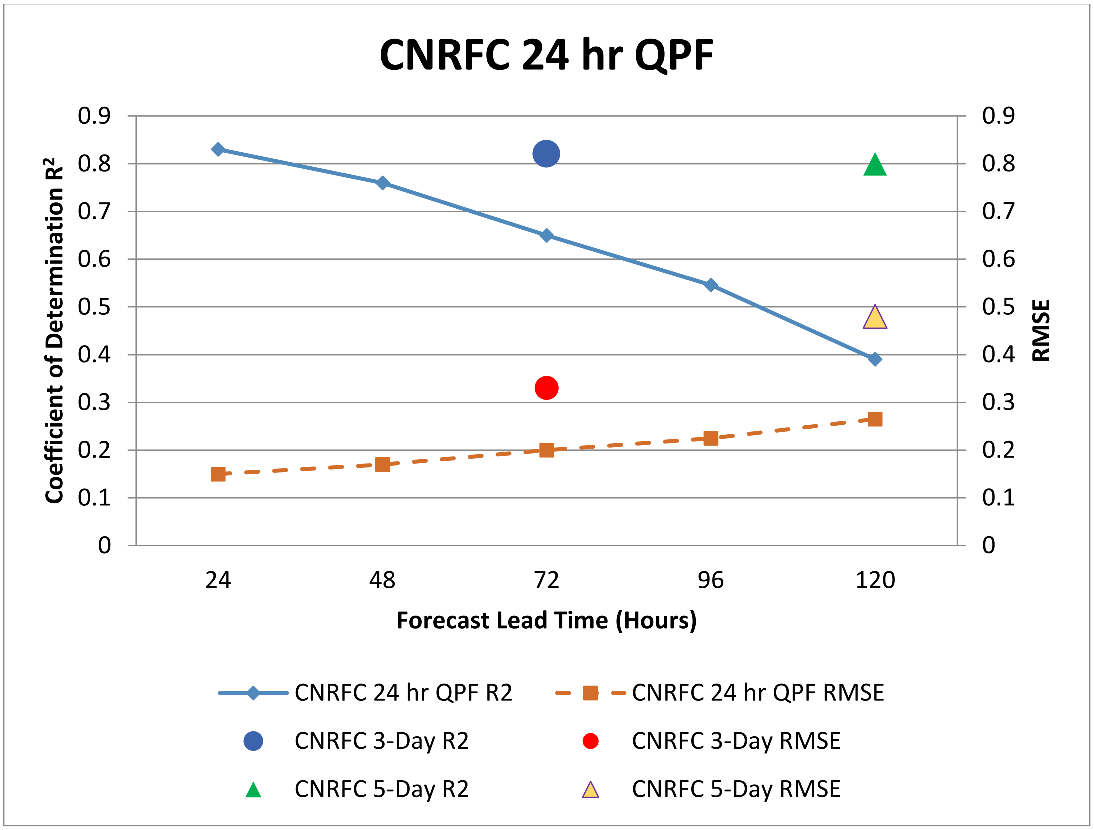

Figure 4.2 Coefficient of Variation (R^2) and RMSE for 24-hr CNRFC QPF. In addition, the values for the day 3 and day 5 cumulative QPFs are shown. The R^2 values for the 3-day and 5-day totals indicate very high predictive accuracy, similar to the day 1 24-hr forecast, indicating that these 3 and 5 day totals remove much of the timing errors that contribute to the lower R2 values for the 6 and 24-hr forecasts out through time.

Given the importance of these 3 and 5-day total rainfall forecasts CW3E researchers determined the trends in these forecasts over the period of record. Figures 4.3 shows the trend in mean error for observed rainfalls of 5 or more inches in 5 days. The plot shows a decrease in under-forecasting these rainfall amounts, with the mean error trending to a near zero bias over the past two years. It has not been determined if these trends are statistically significant given the rather small sample size of these rainfall events but suggests both the models and the forecaster can identify these events better now than in the past.

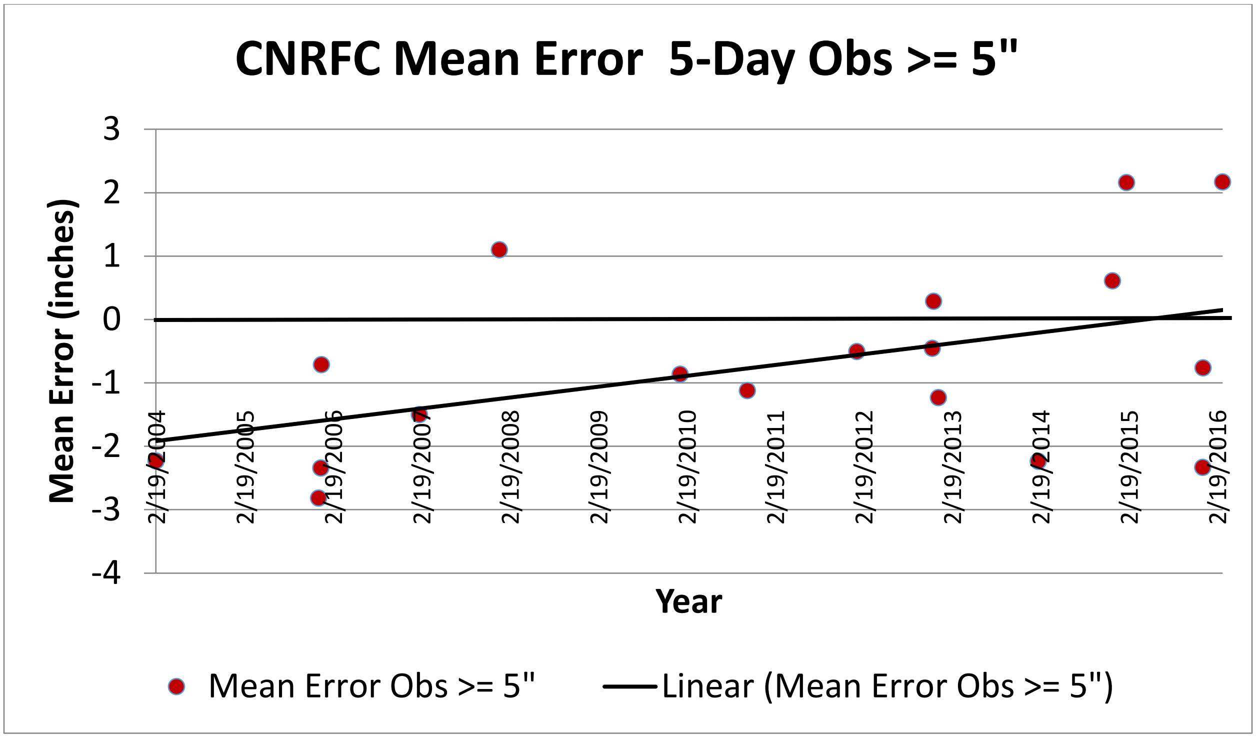

Figure 4.3 Trend in mean error (bias) for 5-day total QPF from CNRFC for observed values at or above 5 inches. The trend in mean error indicates improvement from what was a low bias of almost 2 inches for these events to a near zero bias as of 2016.

Certain rainfall rate thresholds alert the reservoir operator to the need for heightened monitoring. These values are 0.5”/6hr and 1”/24hr as defined in the WCM. In addition, it was noted earlier that 2”/24hr can be associated with large flows (average daily flows > 2500 cfs at Ukiah and thus flows at or above 8,000 cfs Hopland) that can restrict release rates. The skill in forecasting these threshold amounts are demonstrated using the Probability of Detection (POD), the False Alarm Rate (FAR), and the Critical Success Index (CSI). This is done using a simple 2x2 contingency table as shown in Table 1.

Table 4.1. Contingency table of the four possible outcomes for categorical forecasts of a binary (yes/no) event.

Events	**Observed (O)**	**Not observed**
Forecast	Hit (H)	False alarm (F)
Not Forecast	Miss (M)	Correct rejection (CN)

When an MAP threshold, e.g. observed >=1"/24hr, and this threshold is correctly predicted, a hit (H) occurs. When an MAP has a predicted event that is not observed, a false alarm (F) occurs, and when an MAP has an observed event that is not predicted, a miss (M) occurs. Within this context, the POD is the ratio of the number of correct forecasts (H) to the number of observed events (H+M) and the FAR is the ratio of the number of false alarms (F) to the number of forecasts made (H+F). The CSI is the ratio of the correct forecasts (H) to all events either forecast or observed (H+M+F). All three metrics range from 0 to 1, with 1 being perfect POD and CSI scores, and 0 being a perfect FAR score. Figure 4.4 shows the POD, FAR, and CSI values out to 120-hr lead time for the CNRFC 6-hr forecast MAPs for greater than or equal to one-half inch in 6 hours. For comparison, the WPC's record CONUS 6-hr QPF CSI scores for .5in or greater for the first 12 forecast periods for the CONUS averaged over the cool season (Oct.-Apr.) are shown (http://www.wpc.ncep.noaa.gov/html/6hrQPFrecords.htm). The CNRFC CSI scores are very near or above these record values through almost the entire 72-hr forecast period issued by WPC. The CNRFC 36-hr forecast is where the POD and FAR are equal, meaning the forecast is just as likely to be a hit as an over-forecast of this threshold amount. Figure 4.5 shows the skill scores for 24-hr MAPs at or above 1 inch for lead-times of 1 to 5 days. Also shown for comparison is the Consensus (CONS) NWP CSI derived by averaging all available models for each forecast lead time for all available days during the period December 2014 to April 2016. CONS can be considered a multi-model ensemble. These results were derived using the NWS Graphical Forecast Editor (GFE) software as described by Reynolds et al., 2016. The day 1 and day 2 CSI values for CNRFC exceed the WPC records for the cool season October through April for the CONUS (http://www.wpc.ncep.noaa.gov/html/QPFrecords.htm). The CSI for the CNRFC matching the period of the CONS model is also shown. The values are higher than both the CONS model and the 16-year sample as well as the WPC records out through day 3 indicating possible improvement in skill in forecasting these events. The sample size however is rather small so this conclusion should be considered preliminary. The POD and FAR are equal at about day 4.5. Figure 4.6 shows the skill scores for the CNRFC 24-hr MAPs at or above 2 inches. The CONS is also shown for this threshold using the same time period as Figure 4.5. It is again noted that the CNRFC CSI values using the same sample period of December 2014 to April 2016 as the CONS model show higher CSI scores out through day 5. The CNRFC CSI values for day 1 and day 2 16-year sample are at or above the record monthly cool season 2 inch CSI values for WPC day 1 forecasts for the CONUS of 0.42. The POD and FAR lines cross at 3 days but remain close out to day 4. It should be noted that the CSI values for the 2-inch threshold for the CNRFC MAP forecasts for the last two winters are higher than the corresponding 1-inch values. It also shows higher skill for forecasting 2 inch or greater rainfall over the past two winters than the larger 16-year sample and confirming the trend seen in Figure 4.3, indicating improved skill in forecasting heavier rainfall events.

4.3 Conclusions

It was noted the CSI values for this study using the various thresholds were at or above record levels reported by WPC for the CONUS for the cool season. It has also been reported (Charba et al., 2003 and Sukovich et al., 2013) that the CNRFC had higher CSI scores then most other areas of the country for almost all thresholds examined for the cool season. In fact, the CSI results reported here for the day 1 and day 2 CNRFC 2”/24hr exceed the values for the entire CNRFC domain, as shown by Sukovich for the top 1% of cases (1.8”/24hr) for the 2001-2011 data set examined. These higher skill values for the CNRFC are a result of the strong orographic nature of the precipitation, which provides better location and intensity of the precipitation over the Lake Mendocino watershed. This makes the FIRO project well suited for testing along this region of the west coast, where cool season QPF forecasts have at or near the highest skill of anywhere in the CONUS. Given the limitations of CSI and the difficulty of quantifying how its value may impact decision making, the POD and FAR were used to qualitatively assess where skill may drop off for the thresholds evaluated: 0.5”/6hr, 1”/24hr, and 2”/24hr. When the POD falls below the

FAR one could assume that the forecast may be less reliable. This occurs generally between 2.5 and 4 days for each of the forecast thresholds examined. There is also an indication that the skill for the 2”/24hr is at or above that of 1”/24hr, especially for the past two winter seasons. However, this may be impacted by sample size and should be considered preliminary. One final note is that the CSI values for 24-hr amounts for 3 in or greater analyzed for 3 land-falling ARs showed much higher skill than reported by Ralph et al., 2010. These results are included in a paper to be submitted (Reynolds et al., 2016) to J. Hydrometeorology.

These results now provide a baseline by which improvements in NWP and CNRFC forecasts can be compared against as we move forward with FIRO. This will be especially important as the West-WRF model comes on-line and annual analysis of its skill can be compared to these historic values. As noted it was determined that up to 5-days lead time is required for determining potential high runoff events. The results highlighted here indicate that there may be sufficient accuracy when looking at 5-day volumes and not individual 6 or 24-hr forecasts out to 5-days. This would indicate that there is fair confidence in utilizing a 5-day inflow QPF forecast to indicate potential runoff but less confidence in getting the peak inflow right given this is strongly a function of the 6-hr rain rates. Thus future efforts should be placed on improving the models ability to better forecast the timing and intensity of AR landfalls which will improve the 6-hr forecasts that are critical for obtaining accurate timing and intensities of peak inflows.

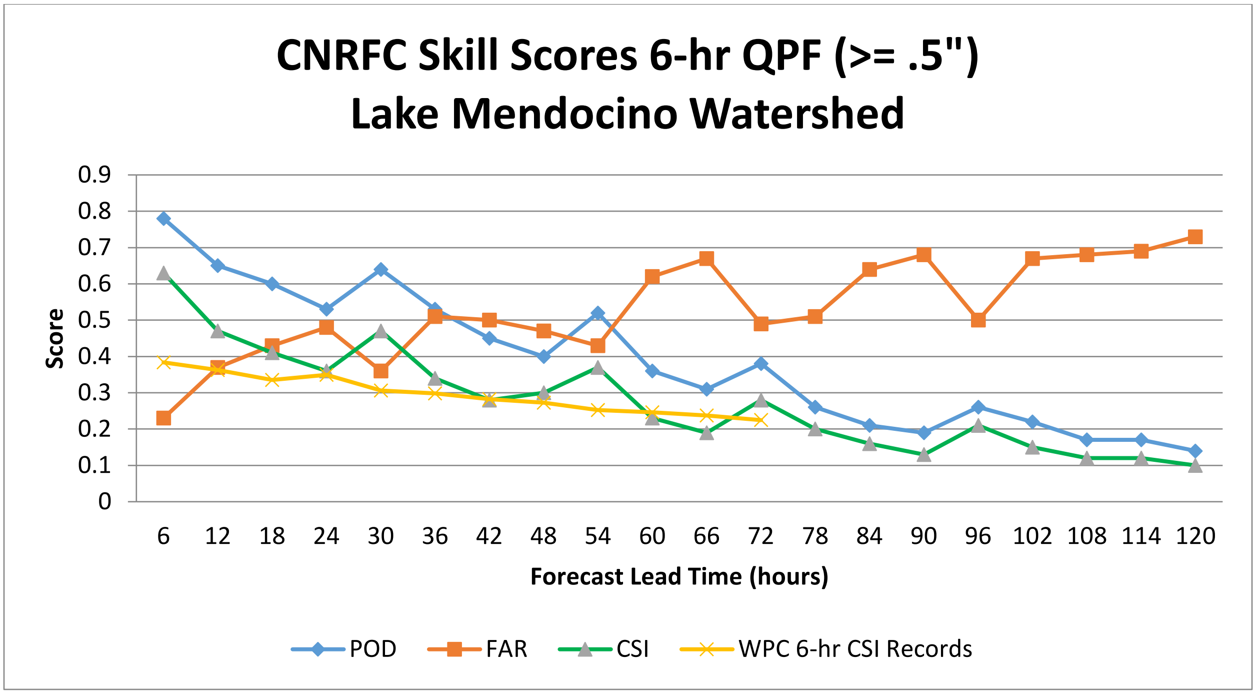

Figure 4.4 Skill scores for CNRFC 6-hr QPFs at or greater than .5 inches in 6 hours versus lead time. The plot shows the rather steep and continuous decline in skill values with a crossover in the POD and FAR at about day 2.5. This would imply less reliability of the 6-hr forecasts and thus streamflow forecasts beyond this time frame. The WPC 6-hr cool-season records for >= .5 " for the CONUS are plotted for comparison.

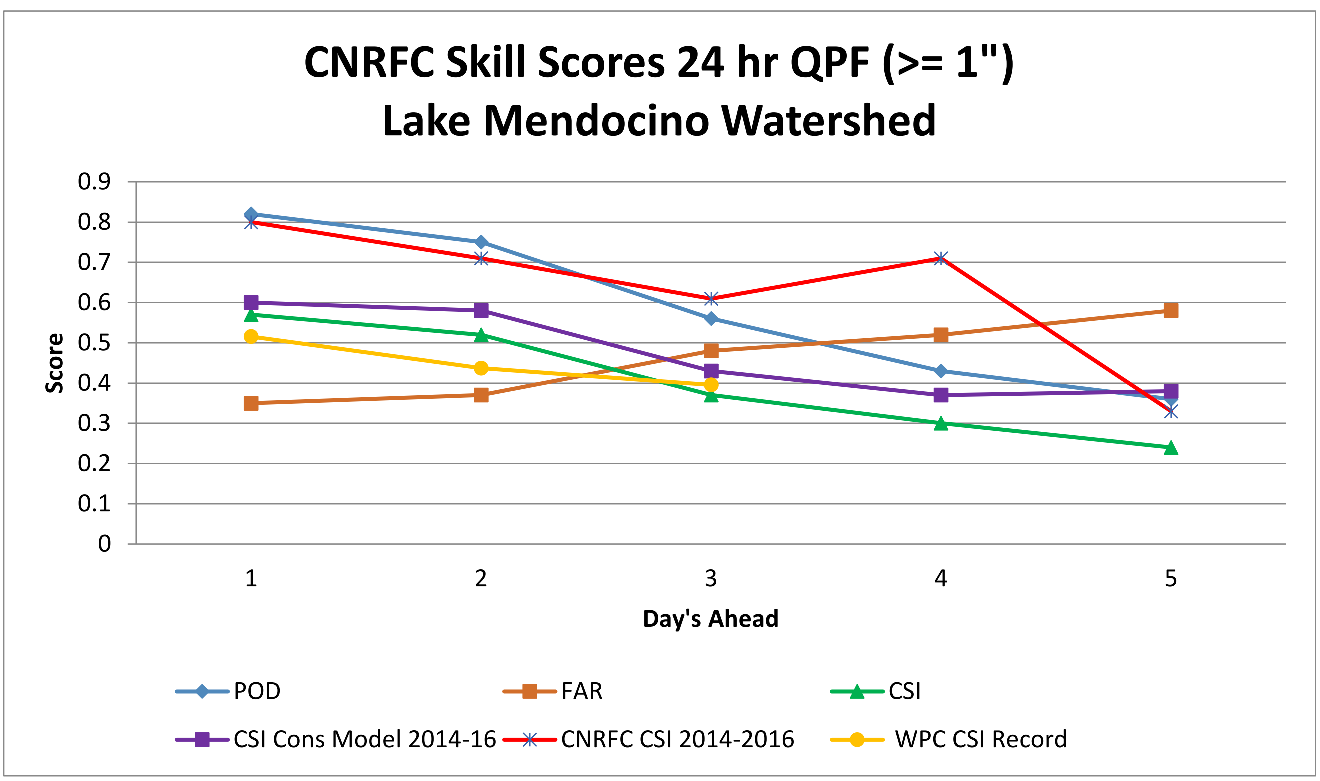

Figure 4.5 Same as Figure 4.4 but for observed MAP greater than or equal to 1 inch in 24 hours versus forecast lead time. The plot indicates that the 24-hr QPFs add about one-day lead time or to 3.5 days versus the 6-hr QPFs. This is again a qualitative assessment using the point where the POD and FAR cross. Comparison of the CONS model to the CNRFC historical values shows the CNRFC is adding value to what has been identified as the "best" model guidance. The plot also indicates that the most recent two-year forecasts from the CNRFC are improvements over the 16-year performance at all led times and well above the WPC cool-season records for the CONUS.

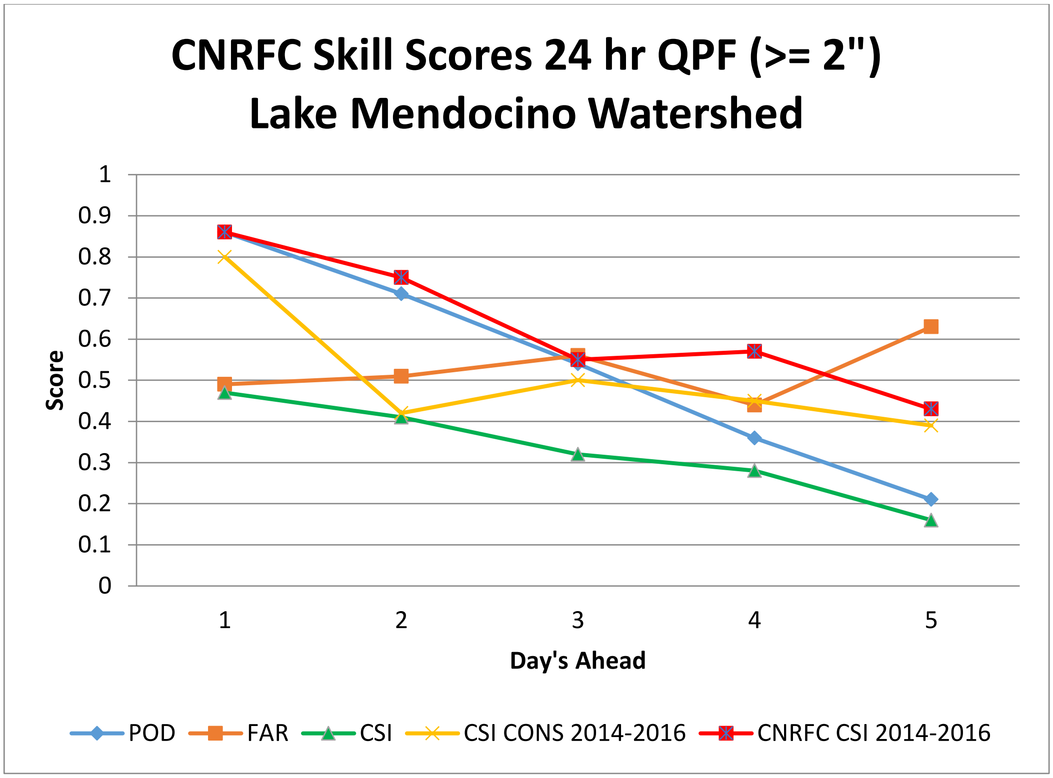

Figure 4.6 Same as Figure 6.5 but for observed MAP greater than or equal to 2 inches in 24 hours versus lead time. Results are similar to those described for the 1 inch or greater amounts. It is however noteworthy that theses 2 inch or greater skill scores are at or above the 1 inch or greater skill using the CSI score. It is also noteworthy that the CSI scores for the CNRFC show a significant improvement over historical skill for this rainfall threshold. Although sample sizes are small this suggests, as Figure 6.3 showed, that skill is improving for the more extreme rain events.

Demargne, J. and others, 2014: The science of NOAA's Operational Hydrologic Ensemble Forecast Service. *Bull, Amer. Meteor. Soc.,* **95**, 79-98.

Charba, J. P., D. W. Reynolds, B. E. McDonald, and G. M. Carter, 2003: Comparative verification of recent quantitative precipitation forecasts in the National Weather Service: A simple approach for scoring forecast accuracy. *Wea. Forecasting*, **18**, 161–183.

Ralph, F. M., E. Sukovich, D. Reynolds, M. Dettinger, S. Weagle, W. Clark, and P. J. Neiman, 2010: Assessment of extreme quantitative precipitation forecasts and development of regional extreme event thresholds using data from HMT-2006 and COOP observers. J. Hydrometeor, **11**, 1286–1304.

Reynolds D. W., S. Sellars, F.M. Ralph, D. Kozlowski, and R. Hartman: 2016: An analysis of quantitative precipitation and streamflow forecasts to assess the viability of forecast informed reservoir operations for Lake Mendocino in Northern California: Part I Quantitative Precipitation Forecasts. Submitted to J. Hydrometeor.

Reynolds, D. W., T. Coleman, D.J. Gottas, and T. LeFebvre, 2015: Utilization of Real-Time Vineyard Observations to Produce Downscaled Temperature Forecasts for Frost Protection Operations. *J. Operational Meteor.,* **3** (1), 1–7, doi: http://dx.doi.org/10.15191/nwajom.2015.03##.

Sukovich, E. M., F. M. Ralph, F. Barthold, D. W. Reynolds, D. R. Novak, 2014: Extreme Quantitative Precipitation Forecast Performance at the Weather Prediction Center from 2001 to 2011. *Wea. Forecasting,* ***29****,* 894-911.

5.0 Skill in Forecasting No Significant Rainfall (no AR landfalls) Over the Lake Mendocino Watershed

5.1 Introduction

From a water supply standpoint, there may be more benefit in forecasting no significant rainfall with high reliability then the more extreme rainfall events. This is because water can be stored above the flood pool during the rainy season if there are reliable forecasts that no significant rainfall/runoff will occur at least over the next 5-days as noted in Section 4.

5.2 Analysis

The CNRFC MAP forecasts were analyzed for situations when one inch or less of precipitation was forecast on a given day from the day 1 through day 5 forecast, and one inch or greater was observed on that day. Table 5.1 shows the number of hits, misses and false alarms for this forecast category. From a reservoir operator's perspective, one would be concerned with any large miss as this might compromise dam safety if the reservoir was well encroached into the flood pool (increased water supply storage). Table 5.2 shows the number of missed forecasts and the mean error when the day 1, 3, or 5 forecast was for less than 1 inch on the verification day and the forecast error was greater than 1 inch. The mean error was just over 1 inch. A unit hydrograph can be used to estimate the runoff from this watershed for this type of error. *The unit hydrograph can be defined as the direct runoff resulting from one* unit *(here one inch) of effective rainfall occurring uniformly over that watershed at a uniform rate over a unit period of time*.

5.3 Conclusions

It was noted in Section 2 that 4-7 days is required to assure that releases made from COY dam are past vulnerable locations downstream such as Guerneville. If there is a forecast of no significant rainfall in next five days no pre-releases would be made within a time frame to make sure those releases are past Guerneville. The closer you get to the event when significant rainfall is forecast makes it more difficult to make pre-releases without contributing to larger flows downstream. Considering the errors noted in Table 5.2 how much additional inflow might be expected that was not predicted? Using a unit hydrograph estimate for the runoff from just over an inch of rainfall in 24 hours for the Lake Mendocino watershed would yield a daily runoff of ~3000 cfs or ~6000 ac-ft. This amount of water could be released safely in under 2 days. More significant are the maximum errors noted. The 3-inch error on a day 5 forecast occurred on 1/25/2008. The inflow from this storm was 2400 cfs per day or ~4700 ac-ft. Again, this water could have been released in under one day assuming no additional rainfall for a few days and Hopland is below 8,000 cfs. Using the NWS Atlas 14 data for the Lake Mendocino watershed

(NWS, 2016) yields a recurrence interval for 3 inches per day of between 1-2 years. One might expect that a more serious missed forecast would be a 25 to 50-year event occurring when no significant rainfall was forecast. The 25 and 50 year 1-day recurrence interval storm is 6 to 7 inches. The largest 1-day MAP observed on the watershed for records dating back to 1948 was 7.06 inches on 12/22/1964, an historic flood in northern California. This yielded almost 30,000 ac-ft of runoff into the reservoir in a single day. Assuming that the reservoir was 10,000 ac-ft encroached into the flood pool, this runoff would push the reservoir to near the top of the flood pool. Based on the 16-year historical forecast record, nothing close to 7" forecast error has occurred for lead times of 1 to 5 days.

Table 5.1. Number of misses per specified forecast lead-time along with the mean and maximum error for CNRFC forecasts of less than or equal to 1 inch/24hrs with a greater than a 1 inch forecast error. The date of the top three forecast errors is provided.

	# Forecasts	Hits	Misses	False Alarm
Day 1	5417	5189	28	70
Day 2	5417	5191	40	68
Day 3	5417	5179	67	80
Day 4	5417	5186	90	73
Day 5	5417	5181	101	78

Table 5.2. Number of misses per specified forecast lead-time along with the mean and maximum error for CNRFC forecast of less than or equal to 1 inch/24hrs and more than 1 inch was observed with greater than a 1 inch forecast error. The date of the top three forecasts errors are provided.

Forecast Lead-time Days	**# of Misses**	**Mean Error(in)**	**Maximum Error (in)**	**Dates of top 3 misses** **Bold indicates AR** **Ralph et al, 2013**
Day 5	46	-1.35	3.01	**1/25/2008 -3.01**" **12/21/2015** -2.76 2/16/2004 -2.61
Day 3	18	-1.22	1.79	11/21//2001 -1.79

				2/16/2004 -1.68 **1/25/2010 -1.65**
Day 1	4	-1.11	1.18	2/12/2000 -1.18 4/16/2000 -1.10 2/19/2002 -1.08

6.0 An Analysis of Streamflow Forecasts to Assess the Viability of Forecast Informed Reservoir Operations for Lake Mendocino in Northern California: Preliminary Results

6.1 Introduction

This verification analysis focuses on forecast inflows produced by hydrological models based on the CNRFC's Quantitative Precipitation Forecast for Lake Mendocino. In order to evaluate hydrologic inflow forecasts for Lake Mendocino, we used verification measures, such as the Root Mean Square Error and the Critical Success Index (CSI) applied to a forecast archive from 2005 to 2016 issued daily beginning at 1200 UTC and extending out 5 days.

6.2 Analysis

A daily hydrological forecast (streamflow in 1000s cfs) data archive was provided by the CNRFC from January 2005 to May 2016. The forecast data was produced daily for twenty 6-hour time increments beginning 18Z for each day on the day stated. There are therefore 20 forecast ordinates (4 forecasts/day x 5 days) and observed values provided for each forecast date. We evaluated 2850 rainy season daily streamflow forecasts (October to May) in all for Lake Mendocino from the forecast data archive.

For forecast verification purposes, we chose to accumulate the 6 hour forecast increments for streamflow to 24-hour and 72-hour forecast increments and converted them to volumetric units in acre-feet (af), which represents the forecasted storage inflow for a reservoir during the time increment. To do this we used the twenty 6 hour forecast ordinates (4x5 days) and transformed them to five 24-hour forecast ordinates (1x5 days). We then used the 24 hour volumes to produce three successive 72-hour forecast ordinates (1x3 days). We define the successive ordinates as lead-time days for assessing the performance of the forecast.

Figure 6.1. shows the Root Mean Square Error (RMSE) in acre-feet for each of the 5 lead time forecast periods representing 24-hour volume forecasts. The forecast lead time day 1 RMSE is 405 af, increasing to 646 af by day 5. Figure 6.2 shows the RMSE values for the 72-hr volumes.

CSI values for the 24-hour volume predictions at the 90th percentile (1148 af), 95th percentile (1916 af) and 99th percentile (4492 af) and the 72-hour volume CSI values for the 90th percentile (3828 af), 95th percentile (5888 af) and 99th percentile (10624 af) are calculated in order to evaluate the forecast archive for the most extreme events in the forecast archive data set. These percentiles are chosen because they are known to be associated with the largest storm systems that a FIRO strategy would need to assess.

Table 6.1. shows the CSI results for forecast lead time days for both 24-hour volumes and 72-hour volumes. Forecasts for the 90th percentile value for both 24-hour and 72-hour volumes show good CSI values for all forecast periods. The 95th percentile CSI values are lower, especially the 24-hour volumes for all lead time forecast periods and drop to 0.39 for forecast day 5 for the 24-hour volumes. 72-hour volumes maintain CSI values greater than 0.5, except for the last forecast lead time period (day 3) for the 95th percentile. The 99th percentile CSI values are much lower, especially the 24-hour volumes for all lead time forecast periods and drop to .21 for forecast day 5 for the 24-hour volumes and only has a CSI value above 0.5 for lead time forecast day 1. Finally, we compare the CSI values for the 99% 24-hr volume of 4492 ac-ft to the CSI values for the 1"/24hr which is also at the 99%. Figure 6.3 shows the comparison.

6.3 Conclusions

The present study focuses on operational CNRFC forecast archive provided for Lake Mendocino inflow from 2005 to 2015 in order to determine the skill of 24-hour and 72-hour volumetric forecasts. The measure presented include general forecast verification approaches (RMSE) and a binary forecast event approach (CSI). Evaluated forecast skill for both the 24-hours and 72-hour volumes showed surprisingly good results across the board. A summary of the results follows:

1. RMSE increases with forecast lead time for 24-hour volumes and 72-hour. RMSE ranges from 405 af (forecast day 1) to 646 af (forecast day 5) and 1012 af (forecast day 1) to 1206 af (forecast day 3) for the 24-hour and 72-hour volumes, respectively.
2. The 90th percentile value for both 24-hour and 72-hour volumes show good CSI values for all forecast periods.
3. The 95th percentile value for 24-hour volumes shows good skill out to forecast day 3, before the CSI value drops below 0.5 for forecast lead day 4 and 5. The 95th percentile value for 72-hour volumes show good CSI values for forecast lead time day 1 and 2.
4. The 99th percentile value for 24-hour volume skill decreases rapidly past day 1, whereas the 72-hour volumes maintain CSI values above 0.4 for both day 1 and 2 forecast lead times.

Overall, the CNRFC streamflow forecast archive shows skillful forecasts for the 90th percentile forecast events for all lead times. The 95th percentile volumes show some challenges in forecasts past day 3 (72-hour) lead-time, although CSI remains close to or above 0.4 for all periods. The 99th percentile volumes, which represent some of the most extreme events in the dataset, do show skill for day 1 (the first 24-hour period) forecasts, but drops off substantially after that, suggesting that accurate forecasting for the most extreme events continues to be a challenge for Lake Mendocino. This result supports the notion that improvement is needed in forecasting the most extreme events for the region.

Table 6.1. CSI values for the 90th, 95th and 99th percentile inflow volumes. The table is split into 24-hour (top) and 72-hour (bottom) Lake Mendocino inflow volume for five forecast day lead times.

Entire Forecast Archive	24 hour volumes (acre-feet)		
	90%	95%	99%
	1148af	1916af	4492af
Forecast Lead Time (days)	CSI	CSI	CSI
1	0.73	0.61	0.53
2	0.67	0.55	0.29
3	0.62	0.52	0.27
4	0.58	0.45	0.25
5	0.56	0.39	0.21
	72 hour volumes (acre-feet)		
	90%	95%	99%
	3828af	5888	10624
Forecast Lead Time (days)	CSI	CSI	CSI
1	0.66	0.57	0.43
2	0.65	0.53	0.44
3	0.62	0.44	0.34

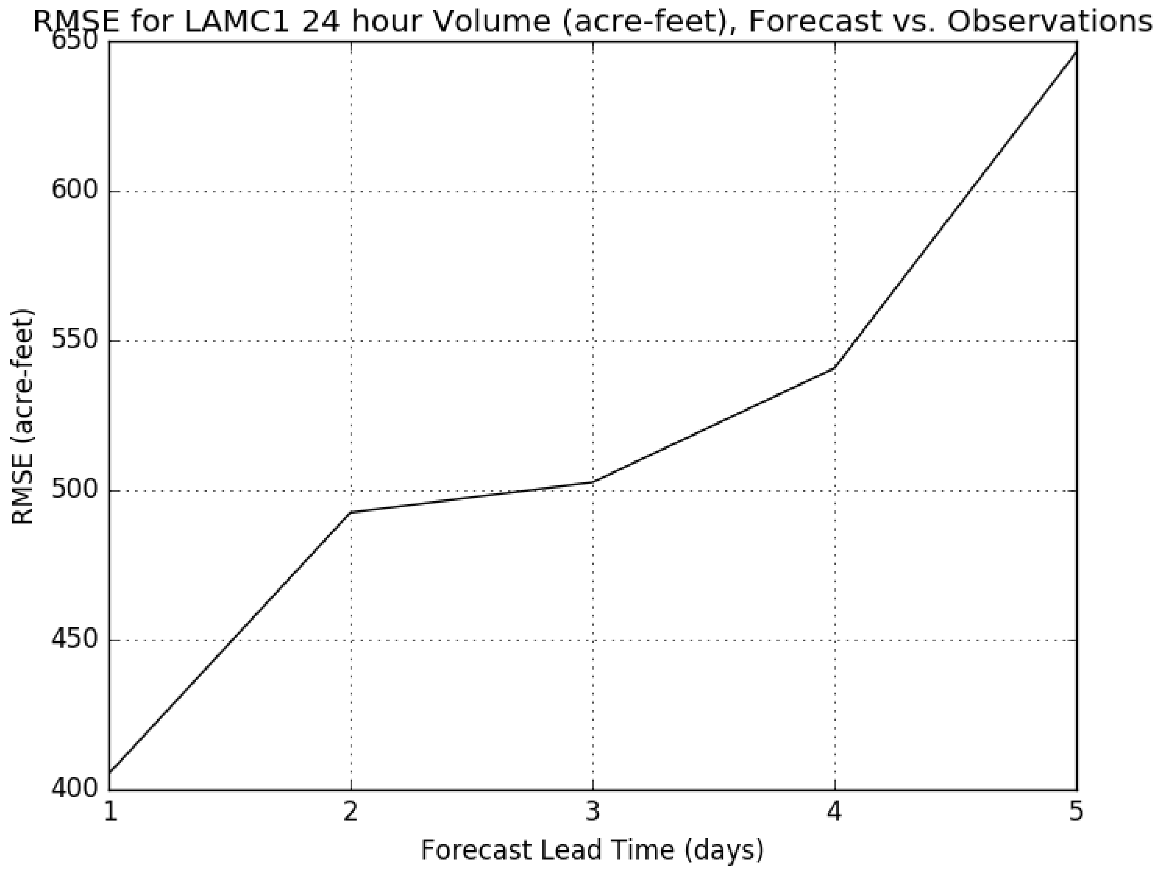

Figure 6.1. Using the entire forecast archive for the accumulated 24-hour inflow volumes, the RMSE for Lake Mendocino volume (acre-feet) is calculated for each Forecast Period (or lead time). A gradual increase in error is seen, although forecast lead time day 2 and 3, only a small increase in seen, while a steadier increase is observed day 4 and 5.

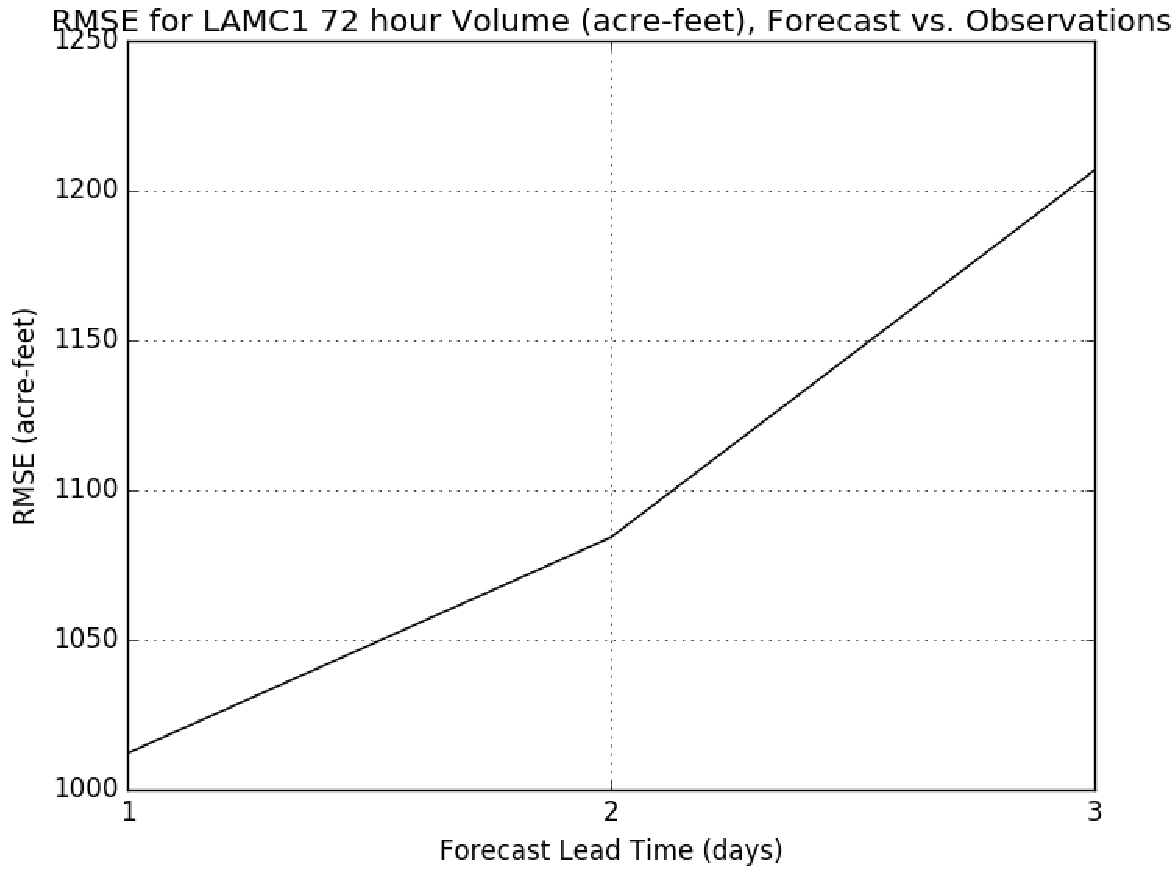

Figure 6.2. Using the entire forecast archive for accumulated 72-hour inflow volumes, the RMSE for Lake Mendocino volume (acre-feet) is calculated for each Forecast Period (or lead time). A gradual increase in error is seen for all lead times.

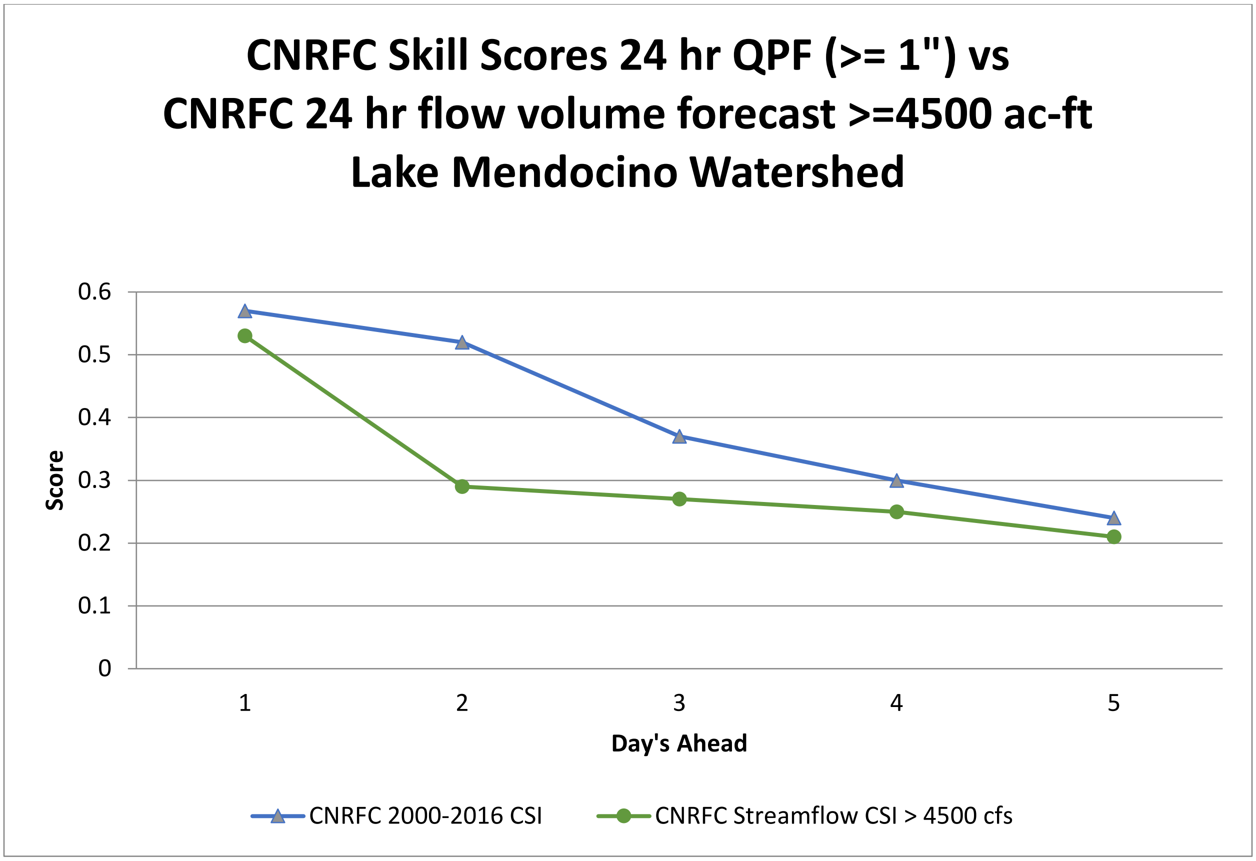

Figure 6.3 CSI values for 2000-2016 CNRFC 24-hr QPFs at or above 1"/24hrs for Lake Mendocino watershed along with the CSI for CNRFC 24-hr streamflow predictions from 2005-2016 at or above 4492 ac-ft. Although the sample years are different it provides a comparison of the inflow forecast skill to rainfall forecast skill out five days. The results suggest that the QPF falls off more gradually than does the inflow forecasts, especially for the day 2 forecast. This suggests the hydrology model may introduce other errors beyond the day 1 forecast that strongly impact the inflow forecast. These results are preliminary and further study needs to be done to compare errors in QPF to errors in inflow forecasts.

7.0 ESRL/PSD NCEP's Global Ensemble Forecasting System (GEFS) Reforecast Version 2 – 1985-2010 Mean Precipitation Verification for Lake Mendocino

7.1 Introduction

Forecasting precipitation is an integral part of streamflow forecasting, water supply planning and flood risk management. The viability of FIRO must look closely at the precipitation forecasts used and determine how the use of improved precipitation and inflow forecasting could enhance water supply and flood risk management. SCWA has developed the Ensemble Forecast Operations (EFO) Model, a risk-based water resource operations model for Lake Mendocino. The EFO Model utilizes hydrologic ensemble forecast information, for a hindcast period of 1985 to 2010, to simulate flood control releases through an assessment of risk of reaching the maximum storage level of the reservoir, while not incurring any additional risk of flooding downstream.

The Meteorological Ensemble Forecast Processor (MEFP) is a statistical model that provides the basis to generate the ensemble of inputs required by the hydrologic models. The MEFP seeks to correct for consistent errors (biases) in the streamflow predictions used for generating the range of ensemble predictions. The MEFP aims to generate unbiased ensemble streamflow traces that capture the skill of the forecasts from different inputs and that preserves the space–time properties of hydrometeorological variables (Schaake et al. 2007a; Wu et al. 2011). The MEFP accommodates several sources of raw forecasts, but for the purpose of the SCWA risk based model, we present a verification of the Global Ensemble Forecast System (GEFS) using the GEFS ensemble mean MAP from 1985-2010.

7.2 Analysis

The CNRFC's Hydrological Ensemble Forecast Service (HEFS) is used to generate the streamflow simulations used by SCWA's risk based reservoir operations model. Precipitation estimates are generated from the NCEP's Global Ensemble Forecasting System (GEFS, Version 10) precipitation dataset (Hamill, 2013) in combination with the MEFP. MEFP provides meteorological forcing for the production of a 61-member hydrological ensemble inflow forecast used as input to the SCWA risk based model. The MEFP is calibrated with both the GEFS 1985-2010 hindcast (days 1-15) as well as the deterministic CNRFC HAS QPF (days 1-3) and utilizes the ensemble mean of the GEFS members rather than the individual members themselves in both the hindcast and real-time operations.

For this verification study, we focus on the ensemble mean of all forecast days and precipitation days (where precipitation is greater than .01 inches) from the GEFS for Lake Mendocino cool season (October to April) from 1985-2010. The observed 6 hour MAP time series (for the lumped area of Lake Mendocino watershed) values are used for comparison with the GEFS MAP mean and the calculated measure of skill is used to assess the CNRFC hydrologic hindcast dataset, which provides the foundation of the SCWA EFO Model.

Using the 2012 version of NCEP's Global Ensemble Forecasting System (GEFS, Version 10), ESRL/PSD Reforecast Project has produced a dataset of historical weather forecasts generated with a numerical model and that consists of an 11-member ensemble of forecasts (Hamill, 2013), produced every day from 00Z initial conditions from Dec 1984 to present. The Reforecast project uses the horizontal resolution of T254 (about 50 km) out to 8 days, and T190 (about 70 km) from 8-16 days for generating past GEFS realizations. Here, we take the GEFS mean precipitation value for the 11 members and use it as the input to the MEFP. This data is used to generate a 1985-2010 hydrology hindcast product used by the SCWA for testing the EFO approach.

Criteria for Lake Mendocino reservoir operations are obtained based on precipitation and streamflow forecasts. One notable criterion is the prediction of 1-inch precipitation in 24 hours, which we verify with the observational MAP data for the hindcast period.

Forecast verification measures provide a way to evaluate forecast information, the observations, or the relationship between the two in a qualitative or quantitative way. Traditional verification measures look at forecast values versus the observed values and calculate numerical scores, which represent the difference between the forecast and observations.

For this study, the GEFS ensemble MAP forecast accuracy is measured using the Correlation of Determination (R^2) and the Root Mean Square Error (RMSE) for day 1 through 16 using the GEFS Hindcast data. The RMSE takes the square root of the average difference between observations and forecasts providing a quantitative value representing the average error of the forecasts. R^2 represents the amount of variance in the observations that is predictable from the forecasts, which describes the relationship between the two. R^2 can also be described as the square of the sample correlation coefficient.

We also utilized a simple 2x2 contingency table comparing the forecast at or above a given threshold to the observed amount to derive skill score measures, which include the Critical Success Index (CSI), Probability of Detection (POD) and False Alarm Rate (FAR). These measures are defined by Joliffe and Stephenson, 2003 and in Section 4 above.

Comparing forecast lead time predictions for the dataset with all cool season days to their corresponding MAP observation values, Figure 7.1 shows a gradual increase in RMSE, starting with .28 inches on forecast day one increasing to .48 inches by forecast day 16. The gradual increase in RMSE provides confidence that the errors are not chaotic and suggests skill that is relative to the lead time of the forecast for Lake Mendocino. The R^2 value decreases with lead time from .64 on forecast day 1 to under .01 at forecast day 16. The R^2 remains above .5 out to the third forecast day, suggesting a linear relationship between the observation and forecast values, although it shows a gradual decrease dropping below .2 by forecast day 8. Figure 7.2 shows the results for only days with precipitation greater than .01 inches. A similar increase in RMSE, starting with.43 inches on forecast day one increasing to .67 inches by forecast day 16. The R^2 value decreases with lead time from .52 on forecast day 1 to under .006 at forecast day 16. For both datasets, day ten and beyond the R2 is so low, that little skill could be inferred from the GEFS forecast and should be used with extreme caution. As enhancements to GEFS are implemented by NCEP and as MEFP is enhanced to better exploit forecast skill in the GEFS, it is expected that future versions will improve the lead time RMSE and R2.

Figure 7.3 shows the results of calculating the CSI, POD and FAR for forecasts of 1-in/24-hours for each of the 16 forecast days. These verification measures show the challenges and benefits in using the GEFS to test FIRO strategies in an ensemble based manner. The CSI value is below .5 for the entire 16-day forecast period for 1-in/24-hour forecasts, yet the major benefit for using the GEFS mean precipitation is that the POD remains above .5 out to forecast day 6, which is indicating that the model is not “missing” a majority of these events. The reason the CSI remains low is because of the high false alarms and is clearly seen in Figure 7.2. The FAR starts at .5 for forecast day one, gradually increasing to the worst value of 1 by day 12. This suggests that there is reliable information up to forecasts day 12.

Figure 7.4 provides a comparison of the RMSE and the R^2 value for the 1985-2010 GEFS v10 forecast data for Lake Mendocino using "All" cool season forecasts and the CNRFC 24-hour QPF for the five-day forecasts for the cool season from 2000-2016. CNRFC forecast scores are used in this comparison as a way to ensure that the GEFS hindcast data is producing forecast skill scores similar to that of the CNRFC forecasters. Figure 7.4 shows that the RMSE scores for the GEFS are significantly higher than the CNRFC with the Day 5 CNRFC RMSE lower than the Day 1 GEFS value. The R^2 values for the GEFS lag behind the CNRFC by about 3.5 days, although the R^2 scores converge by forecast day 5. It should be noted that the rate of drop-off of the R^2 score is smaller for the GEFS then the CNRFC.

7.3 Conclusions

The verification analysis found that the GEFS mean precipitation forecasts for Lake Mendocino are suitable for testing and evaluating FIRO based strategies. Errors increase with lead time, but there is substantial forecast information with the POD remaining greater than .5 with lead times out 6 days for the important forecasts of 1-in/24-hours and the RMSE only increasing by .09 and .11 for cool season forecasts and cool season precipitation days, respectfully. The GEFS lead time skill lags the CNRFC skill by several days, with the CNFRC forecasts also having both lower RMSE and higher R^2 values through 5 days. Caution should be used in using the GEFS mean MAP after day 10 to 12, as the skill for predicting 1-in/24-hour events dramatically decreases with low R^2 values as seen in Figure 7.1 and 7.2. Also, the FAR remains high for all lead time periods, suggesting that over prediction of precipitation is evident in the GEFS mean precipitation data. One other precautionary note is that the hindcast data set has limited both extreme high flows and low flows. Thus, the calibration of the HEFS utilizing this limited data set may contribute to model inflow errors when simulating the more extreme high inflows and low inflows into Lake Mendocino.

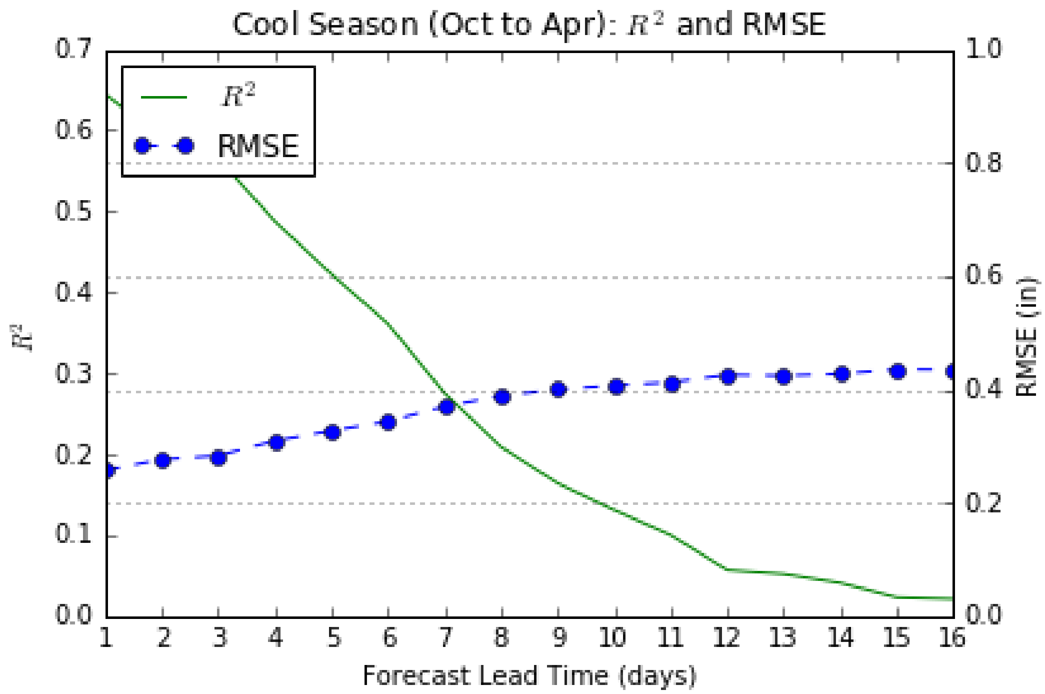

Figure 7.1. The RMSE and the R^2 value for the 1985-2010 GEFS v10 precipitation data for Lake Mendocino, used in the evaluation of FIRO based strategies experimented by SCWA risk based model.

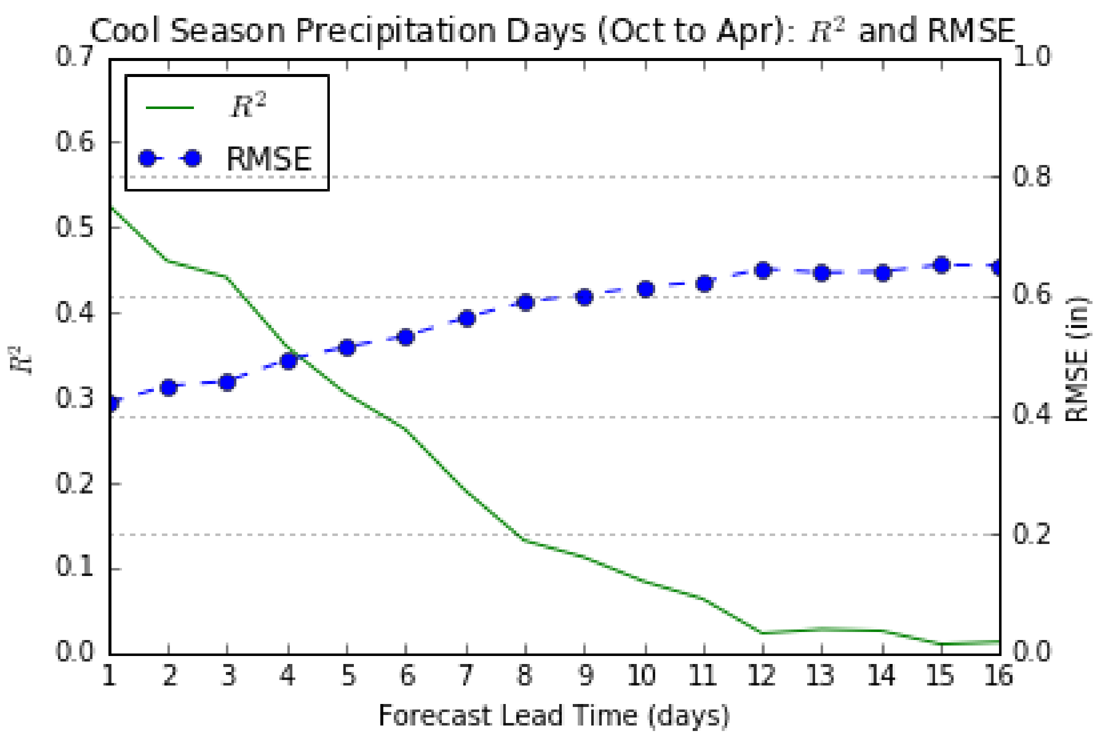

Figure 7.2. The RMSE and the R^2 value for precipitation days (where precipitation is greater than .01 inches) during the cool season (October to April) 1985-2010 GEFS v10 precipitation data for Lake Mendocino, used in the evaluation of FIRO based strategies experimented by SCWA risk based model.

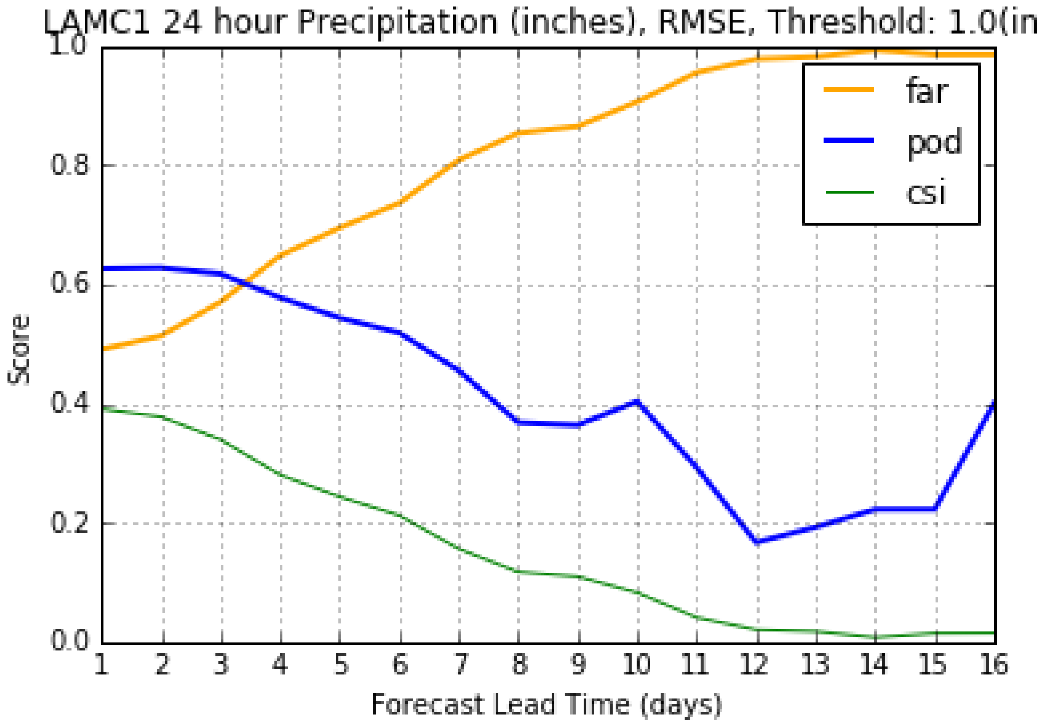

Figure 7.2. The CSI POD and FAR forecast lead time values for 1inch of precipitation or greater (1in CSI, POD and FAR threshold) for the 1985-2010 GEFS v10 precipitation data for Lake Mendocino, used in the evaluation of FIRO based strategies experimented by SCWA risk based model.

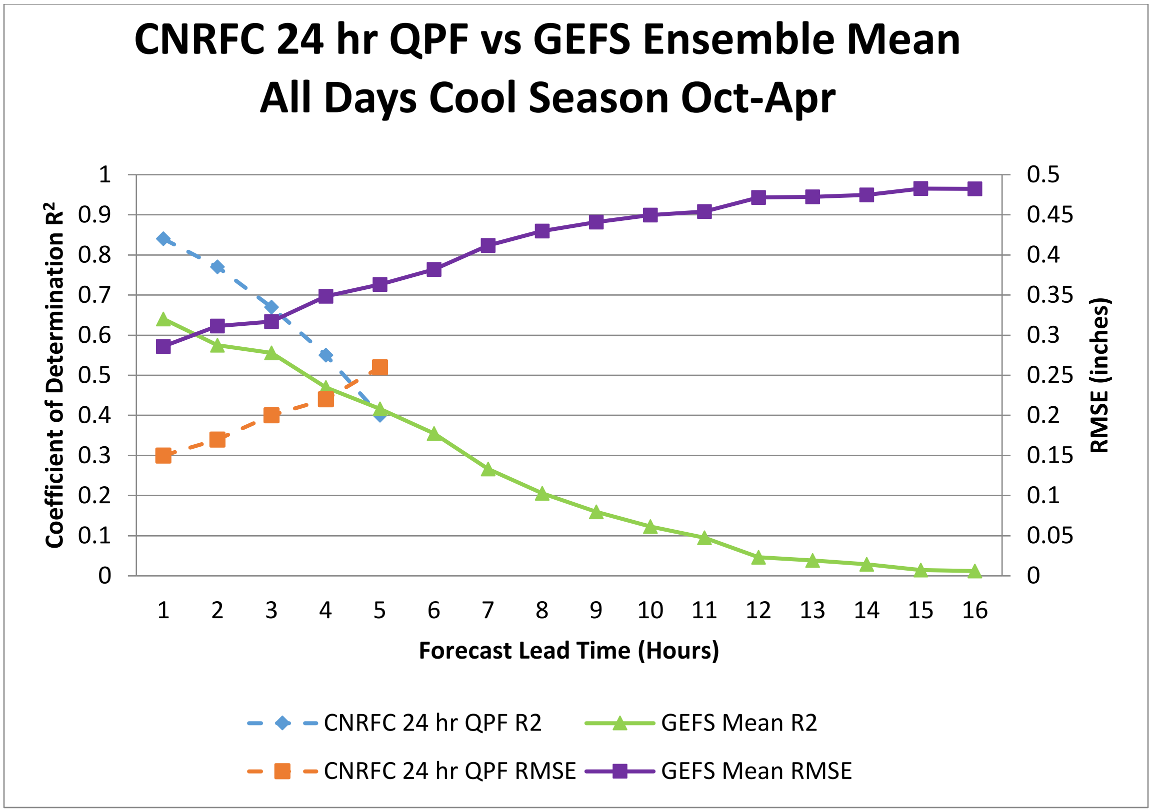

Figure 7.4. A comparison of the RMSE and the R^2 value for the 1985-2010 GEFS v10 cool season precipitation forecasts using all days for Lake Mendocino and the CNRFC 24 hour QPF for the five day forecasts for period 2000-2016. The GEFS v10 data is used in the evaluation of FIRO based strategies experimented by SCWA EFO Model. The CNRFC forecast shows higher accuracy in both R^2 and RMSE through almost the full duration of the CNRFC forecast, five days. This would imply that the operational HEFS should use the CNRFC deterministic forecast through five days instead of three as is currently done.

References:

Hamill, T. M., G. T. Bates, J. S. Whitaker, D. R. Murray, M. Fiorino, T. J. Galarneau, Jr., Y. Zhu, and W. Lapenta, 2013: NOAA's second-generation global medium-range ensemble reforecast data set. *Bull Amer. Meteor. Soc.*, 94, 1553-1565. doi: http://dx.doi.org/10.1175/BAMS-D-12-00014.1

Schaake, J., and Coauthors, 2007a: Precipitation and temperature ensemble forecasts from single-value forecasts. Hydrol. Earth Syst. Sci. Discuss., 4, 655–717.

Wu, L., D.-J. Seo, J. Demargne, J. Brown, S. Cong, and J. Schaake, 2011: Generation of ensemble precipitation forecast from single-valued quantitative precipitation forecast via meta-Gaussian distribution models. J. Hydrol., 399 (3–4), 281–298.

8.0 Importance of Extreme Rainfall Events to Annual Precipitation in the Russian River Basin

8.1 Introduction

Dettinger and Cayan (2014) and Dettinger (2016), have described the importance of the top 5-to 10 percent of heaviest rainfall events that occur in California to the average annual rainfall and to the year-to-year variance in annual rainfall. These studies show that the wettest 5% of rainy days in California contribute about a third of the precipitation but about two-thirds of the variance in water-year precipitation. Here we highlight the impact of extreme rainfall events on the Russian River watershed.

8.2 Analysis

Specifically, for the Russian River basin, contributions from the top 10% of the rainfall events on average make up 40% of the total annual precipitation whereas the smaller events on average make up the other 60%. However, the contributions from the top 10% of the events have almost twice the variance of the smaller storms. Figure 8.1 shows the annual water-year precipitation based on daily averages of Ukiah and Santa Rosa. Plotted are the contributions from the top 10% of rainy days and the contribution from the remaining 90% of rainy days. Contributions from top 10% of wet days explain 81% of variance of the fluctuations of total water-year precipitation. Smaller-storm contributions explain only 62% of total-water-year precipitation fluctuations. Once smoothed with a 5-yr moving average (as in curves in the figure), the top 10% of rainy-day contributions still explain 81% of smoothed total-water year precipitation fluctuations, whereas the smaller-storm contributions explain only 58% of the variance. AR events explain 75% of precipitation variations during the 1948–2014 period when water-year counts of pineapple expresses are available (Dettinger et al. 2011, and updates thereto). Among the wettest days, in the 1998–2008 period covered by the chronology of all AR landfalls in California reported in Dettinger et al. (2011), 48% of the wettest 5% of wet days correspond to occasions with landfalling ARs, despite AR landfalls making up only about 5% of all wet days. Overall then, ARs provide a disproportionate number of the wettest days in California.

8.3 Conclusion

These findings indicate that on a water-year scale (as well as on multi-year time scales) the occurrence (or absence) of very large storms, and especially ARs, dictates the occurrence of most risk of drought in the Russian River basin. Previous studies have shown that these same ARs are the causes of 80% or more of historical floods in the Russian River basin. In practice, FIRO would tend to focus on storm-by-storm management of Lake Mendocino to obtain its water-supply and fisheries benefits, while maintaining current levels of flood-risk management, but the findings above suggest that management of those storms will also relate directly to the large majority of multi-year drought (and pluvial) risks. A focus on the largest storms in the Russian River basin amounts to a focus on the cause of 80% or more of the multi-year fluctuations of the water balance there.

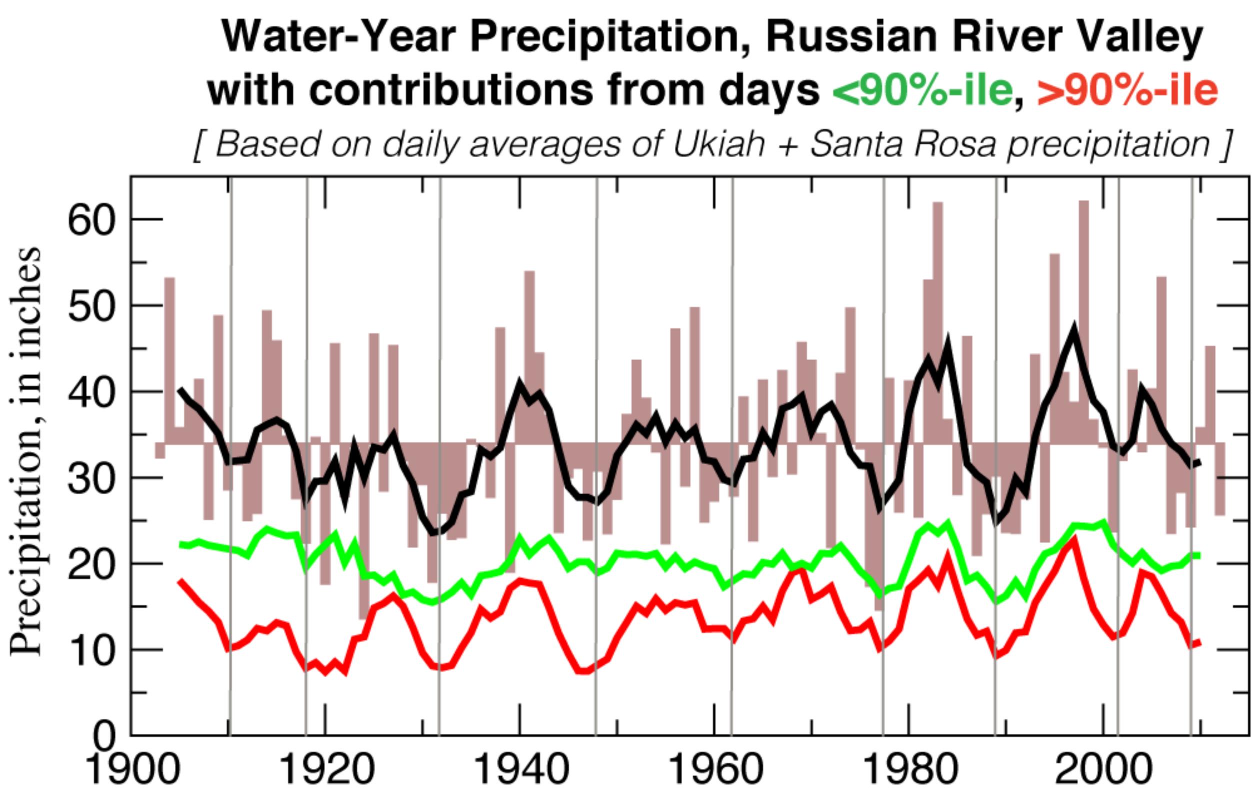

Figure 8.1 Water-year precipitation for Russian River Basin (mean from Ukiah and Santa Rosa gauges) (tan bars), contributions toward water year precipitation from greater than the wettest 10% events (5-year running average - redline) and contribution from the remaining 90 % of the events to water year precipitation plotted as 5-year running average(green)

Dettinger MD, Ralph FM, Das T, Neiman PJ, Cayan D. 2011. Atmospheric rivers, floods, and the water
resources of California. Water 3(2):455–478. [cited May 19 2014]. Available from: *http://www.mdpi.com/2073-4441/3/2/445*.

Dettinger MD, Cayan DR. 2014. Drought and the California Delta—a matter of extremes. San Franc Estuary Watershed Sci 12(2). doi: *http://dx.doi.org/10.15447/sfews.2014v12iss2art4*

Dettinger MD, 2016: Historical and future relationships between large storms and droughts in California. San Franc Estuary Watershed Sci 14(2). http://escholarship.org/uc/item/1hq3504j

9.0 Relationship of upslope water vapor flux and rainfall for land-falling ARs

9.1 Introduction

The climatology of Atmospheric River (AR) conditions at Bodega Bay, CA shown in Ralph et al. 2013 has been updated and increased from 91 AR events (Nov. 2004–May 2010) to 172 AR events (Nov. 2004–May 2016). An AR is defined based on three conditions: 1) integrated water vapor (IWV) must be greater than 2 cm, 2) the upslope water vapor flux in the controlling layer (0.75–1.25 km MSL) must be above 15 cm (m s^{-1}), and 3) these two conditions must be simultaneously met for at least eight hours. One major conclusion of this study was the large role of storm-total upslope water vapor flux during AR conditions in controlling the storm-total rainfall. The original comparison found the total flux and precipitation were well correlated with $r^2=0.75$.

9.2 Analysis

An updated climatology was computed utilizing an additional 6 years of data. The results, Figure 9.1, indicate a slightly lower correlation with $r^2=0.62$. The main reason for this decrease in correlation is the increase in variation in the longer duration events. The update added four long-duration (>31 hours) AR events which all produced high total upslope flux (>800 cm (m s^{-1})) but low total precipitation (<40 mm). It is important to note that three of these four events occurred during June, not during the cool season when the majority of AR events occur in this region. The update also included the most extreme event in the climatology, which occurred 7–10 February 2014, and produced total upslope flux of ~2250 cm (m s^{-1}) and ~330 mm of precipitation (see Section 10 below).

The relationship between AR conditions and heavy precipitation yields the importance of accurate forecasting of ARs. Recent work has focused on developing tools and methods to better interpret model output to increase the accuracy of AR forecasts. One such tool, shown in Figure 9.2, is the AR landfall tool. This tool uses the Global Ensemble Forecast System (GEFS) to show the probability of AR conditions occurring along the U.S. West Coast over the next 16 days. AR conditions are defined as IVT >250 kg m^{-1} s^{-1} (Figure 9.2 a-b), with versions using 500 kg m^{-1} s^{-1} (Figure 9.2 c-d) and 150 kg m^{-1} s^{-1} (not shown) also available. The left panel shows a time-latitude depiction of the fraction of GEFS members that indicate the presence of AR conditions at a given location (shown on map in right panel) at a given time. The right panel also indicates the number of hours at a given location when AR conditions are forecasted by >99%, >75%, and >50% of the GEFS members. The differences between Fig. 9.2a and Fig. 9.2b (also Fig. 9.2c and Fig. 9.2d) indicate the results of a recent upgrade to the product which occurred in March 2016. This upgrade increased the spatial resolution from 1.0° to 0.5°, temporal resolution from 6-hours to 3-hours, added the 150 kg m^{-1} s^{-1}, and created the product for inland locations. Comparisons between the pre- and post-upgrade products indicate the large amount of detail that can gained with an increase in both spatial and temporal resolution. This product allows the user to view a 16-day forecast of ARs over a large geographical domain in one image. The forecasted duration of AR conditions at given locations, the spatial extent of an AR, and the relative strength of an AR can be determined from this product.

9.3 Conclusion

While the updated r^2 value is slightly lower, the result still shows a strong correlation between total upslope water vapor flux and storm-total precipitation, however the variation in total precipitation during the more extreme events illustrates that other atmospheric conditions also play a large role in precipitation production. Current research looks to bridge the gap in our understanding of other factors that lead to this variation in precipitation production.

Ralph, F. M., T. Coleman, P. J. Neiman, R. J. Zamora, and M. D. Dettinger, 2013: Observed impacts of duration and seasonality of atmospheric-river landfalls on soil moisture and runoff in coastal northern California. *J. Hydrometeor*, **14**, 443–459.

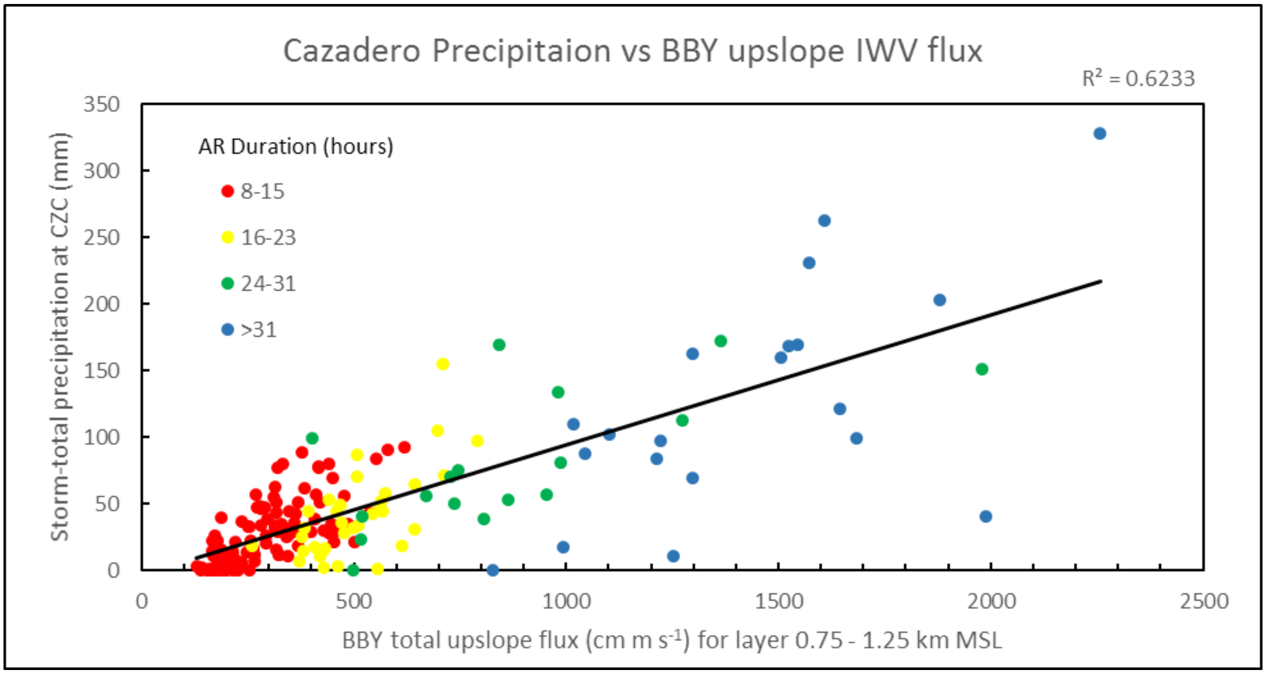

Figure 9.1: Scatterplot of storm-total precipitation at Cazadero, CA vs storm-total upslope water vapor flux at Bodega Bay, CA during AR conditions for 172 AR cases, color coded by duration of AR conditions.

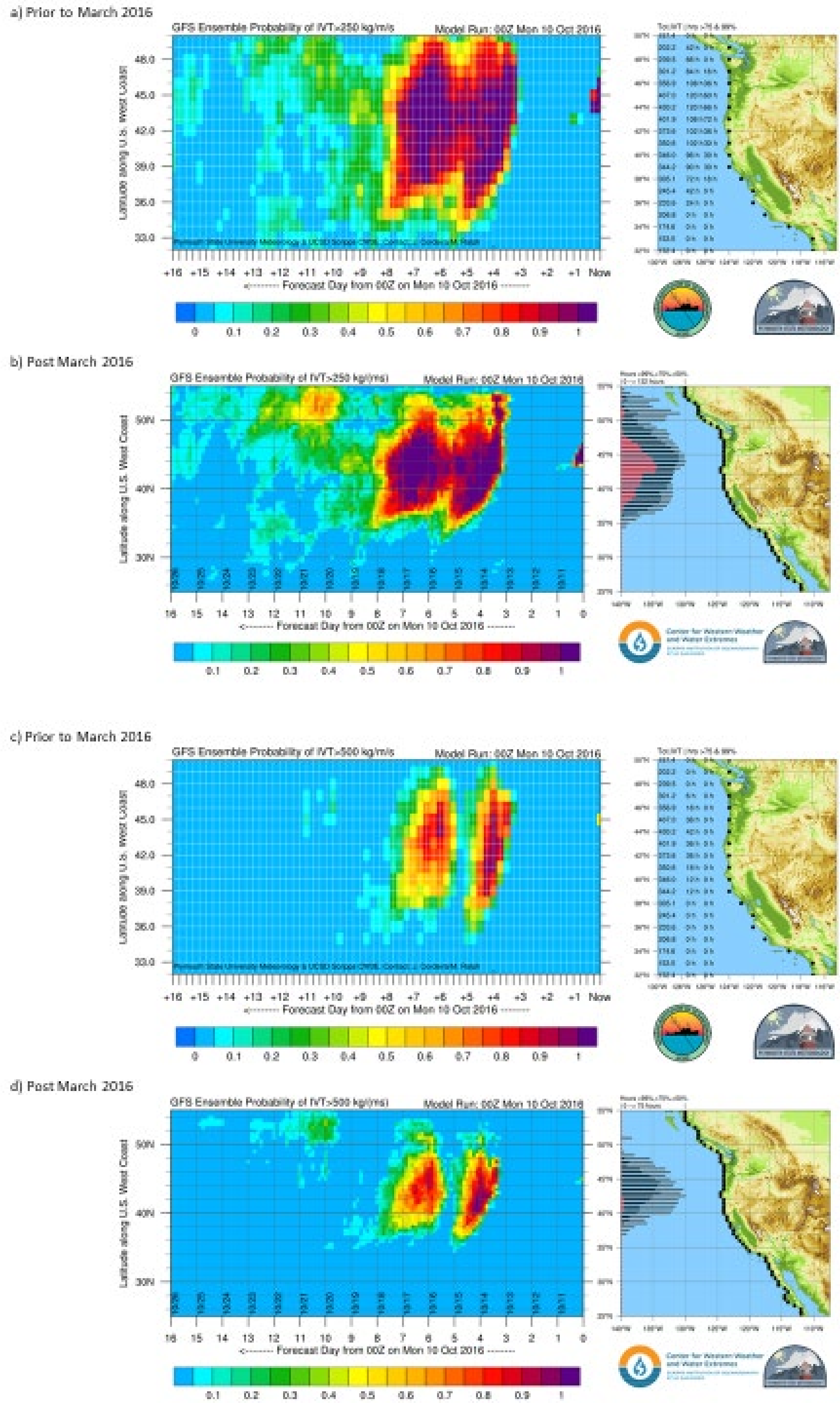

Figure 9.2 The Global Ensemble Forecast System (GEFS) AR Landfall tool prior to March 2016 (a and c) and after March 2016 (b and d) using thresholds of 250 kg m^{-1} s^{-1} (a-b) and 500 kg m^{-1} s^{-1} (c-d). Tool developed and created by Dr. Jason Cordeira, Plymouth State University.

10.0 Impact of frontal waves along Atmospheric Rivers on flood forecasting in Russian River Basin

10.1 Introduction

Mesoscale frontal waves (MFWs) are one mechanism that can significantly degrade forecast skill, but with early identification using existing tools, they can improve the quantification and communication of forecast uncertainty and ultimately improve forecasts as this feature becomes better understood. In general, MFWs slow down the forward movement of AR, impacting the timing and location of the heaviest rainfall at a given location. MFWs can be observed with satellite sensors and appropriately placed ground-based sensors. An example case in early December 2014 is presented here.

10.2 Analysis

Mesoscale Frontal Wave of December 10-12, 2014

Observed with the Special Sensor Microwave Imager (SSMI), MFWs appear as a cusp-like shape along the advancing atmospheric river (Figure 10.1). At the Bodega Bay AR observatory (BBY in Figure 1.1), which is equipped with GPS water vapor and wind profiling capabilities, the MFW signal includes a decrease in low level wind speed, change in wind direction, and decrease in precipitation intensity for a period of several hours after initial AR landfall as seen between the vertical bars shown in Figure 10.2. It is apparent that the wave was not forecast well by the Rapid Update Cycle (RAP) model used to display forecast upslope winds and precipitation (Figures 9.2), while the forecasts of integrated water vapor (IWV) alone remained skillful. The model's inability to identify the MFW can eventually contribute in a false alarm for the extent of flood risk by contributing to errors in quantitative precipitation forecasts (Figure 10.3) and subsequent streamflow forecasts (Figure 10.4). In this event, there was a 10-foot difference in peak flood stage prediction between the predictions on 8 December 2014 and those on 10 December 2014. This over prediction can be partially attributed to the MWF slowing down the onset of the heaviest rainfall. This error in timing along with the over predictions for the peak and tail of the

AR passage contributed to the 10 ft change between 8 and 10 December and the error in the flood stage forecast.

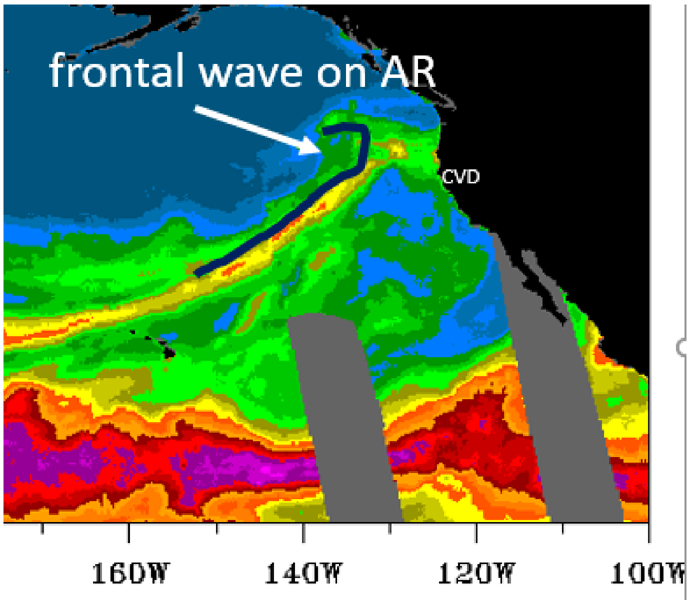

Figure 10.1 SSMI integrated water vapor image for 10 Dec 2014 showing frontal wave along the advancing AR towards the Russian River Basin.

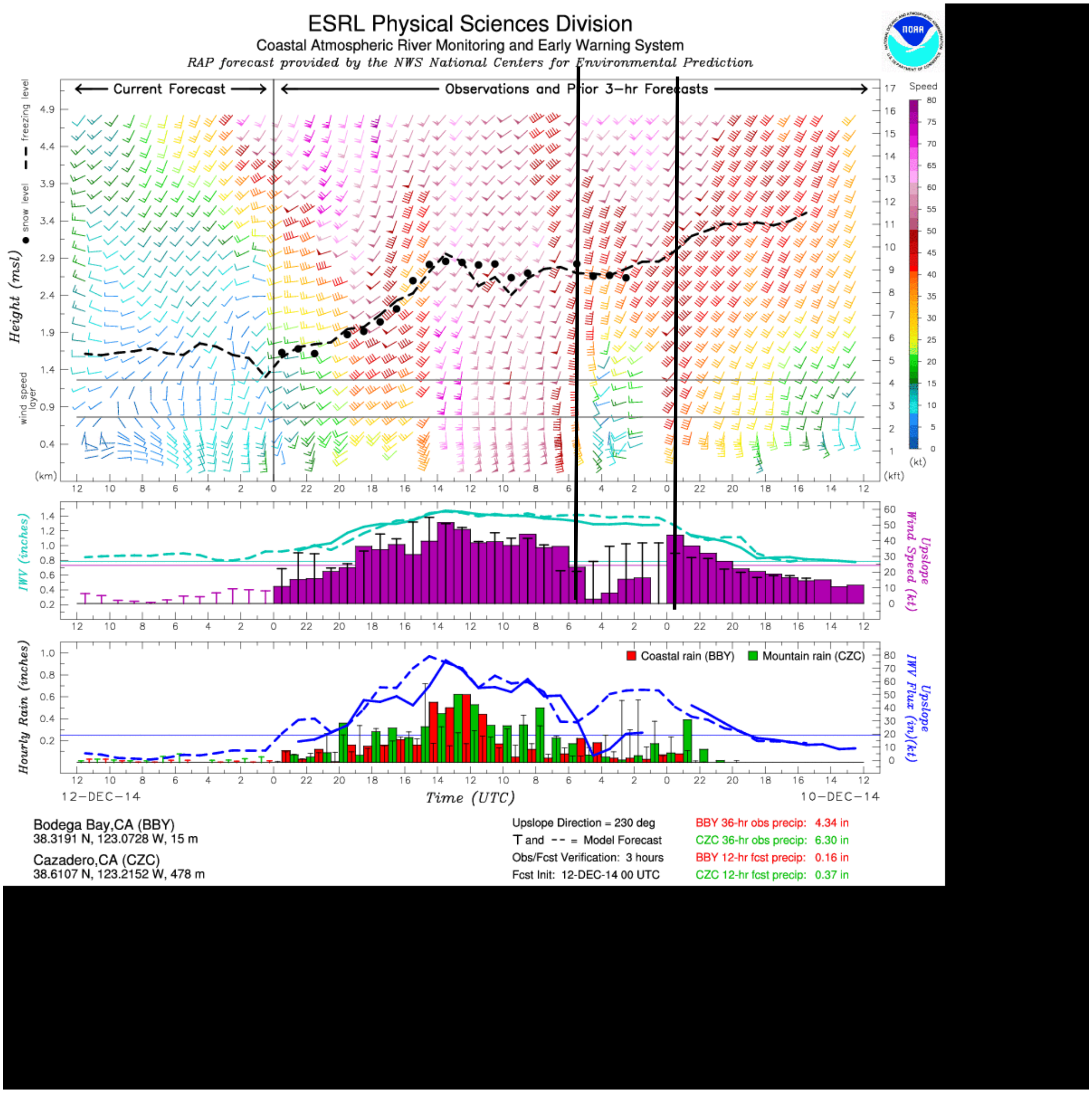

Figure 10.2 ARO observations at BBY and Cazadero (CZC in Figure 1.1) (from 10-11 December 2014 (plot reads right to left with advancing time). Rapid Update Cycle Model (RAP) predictions are included in dashed lines and vertical bars and go through 12Z on 12 December 2014. Black vertical bars on the top winds plot indicate the times where the frontal wave affected AR conditions and associated predictions at the ARO.

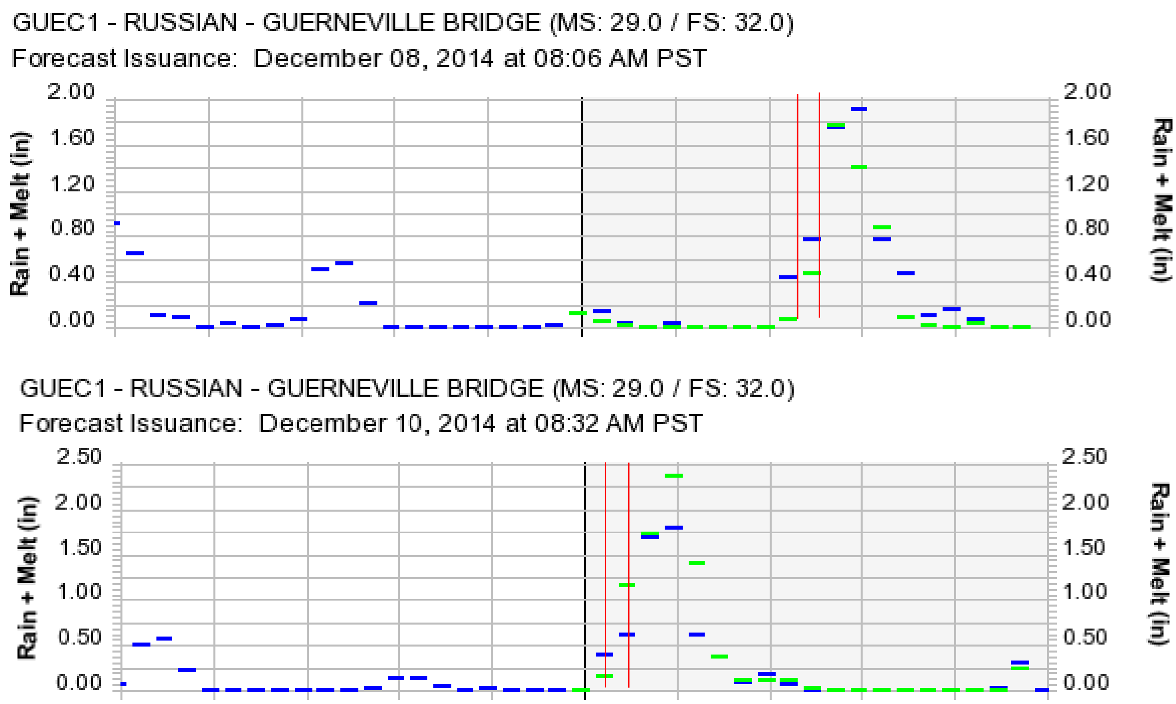

Figure 10.3. Mean Areal Precipitation in 6-hr periods is shown for observed (blue) and predicted (light green) for Guerneville, for the entire basin upstream of the station. A moderate under-prediction on 8 December for the forecast period 0-6Z 10 December (within vertical red lines shown) moves to a significant over-prediction on 10 December during that same forecast period. Time of issuance of the forecast is indicated by the heavy vertical line in the middle of the plots. Plot is from the California Nevada River Forecast Center.

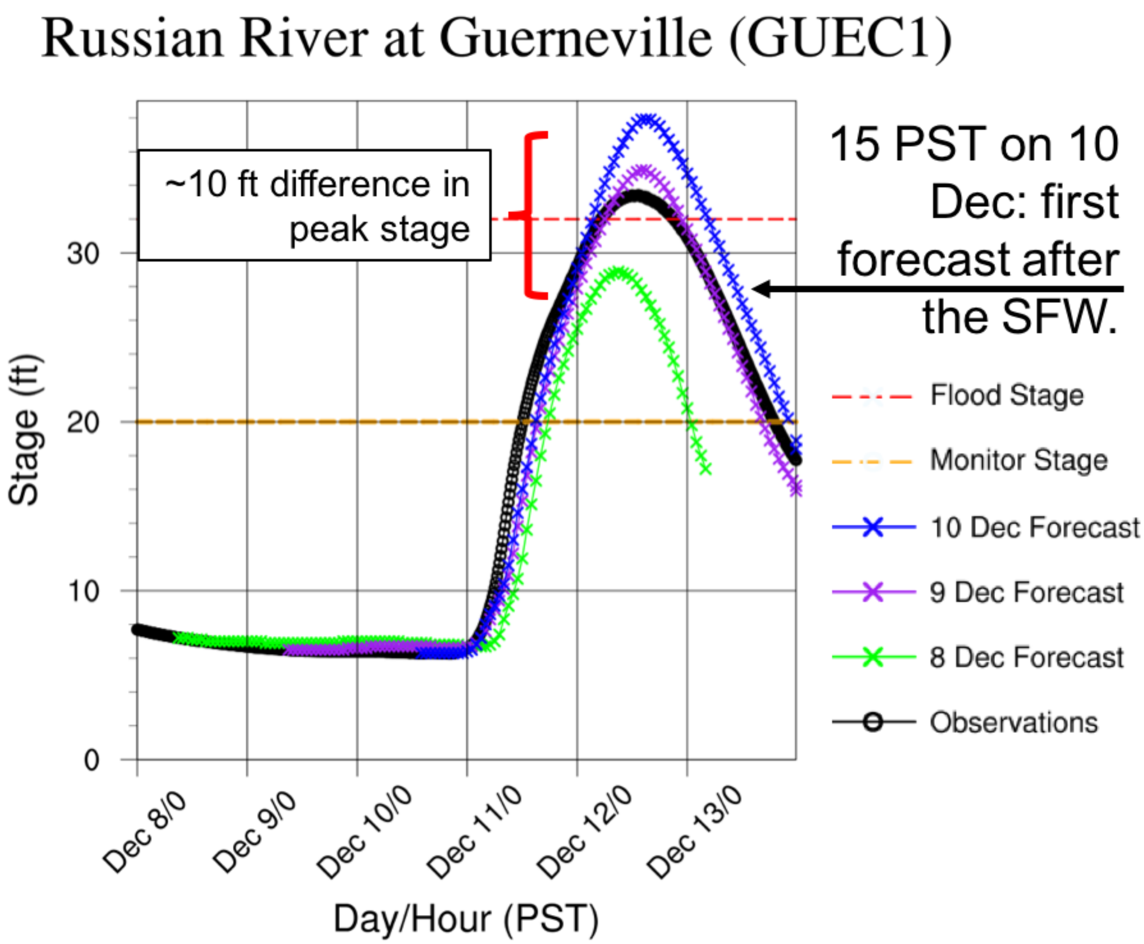

Fig. 10.4 Stage forecasts and observations for 8-14 December 2014 at various lead times. Data are from the California Nevada River Forecast Center. The plot highlights the ten-foot discrepancy in river stage at Geurneville between the forecast issued 8 Dec and 10 Dec 2014. The difference was, in part, attributed to the models not forecasting the impacts of the MFW on precipitation.

<u>February 7-10, 2014 AR Analysis of multiple mesoscale frontal waves</u>

Neiman et al., 2016 have documented both detailed offshore measurements of a land-falling AR using multiple aircraft sampling flights and utilizing the ARO and corresponding observations at the BBY and Cazadero sites. Three transient mesoscale frontal waves modulated the AR environment both offshore and over Northern California. Two of these can be seen in Figure 9.5. These waves stalled the front, thus prolonging AR conditions and heavy precipitation upon landfall. The eventual southward migration of the polar front (as a cold front) marked the end of AR conditions across California. This case again shows the impact of MFWs on downwind orographic precipitation when the upslope IVT is both enhanced ahead of the MFW and decreased by the passage of the MFW. These waves are depicted in Figures 9.5 and 9.6 taken from Neiman et al, 2016. Although no flooding occurred from this multi-day AR event due to dry antecedent soil moisture conditions, this case does show the importance of numerical guidance being able to identify these features and properly forecast their propagation as they move onshore.

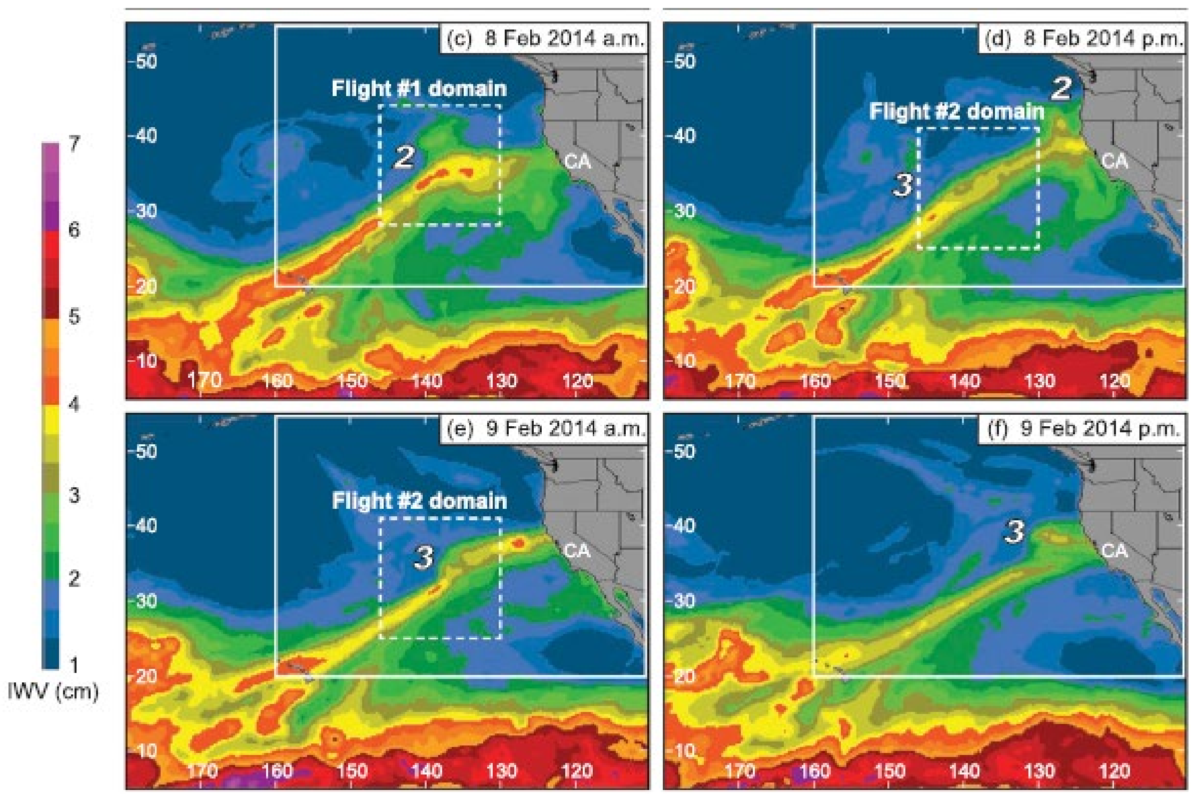

Figure 9.5 (c-f) Composite SSMIS satellite imagery of IWV (cm; color scale on left) constructed from polar-orbiting swaths between 0000 and 1159 UTC (a.m. images) and between 1200 and 2359 UTC (p.m. images) on 8–10 Feb 2014. The dashed white box in (c) and (e) shows the domain of the G-IV flights. The italic numbers mark two of the three frontal waves described in Figures 9.6 and 9.7.

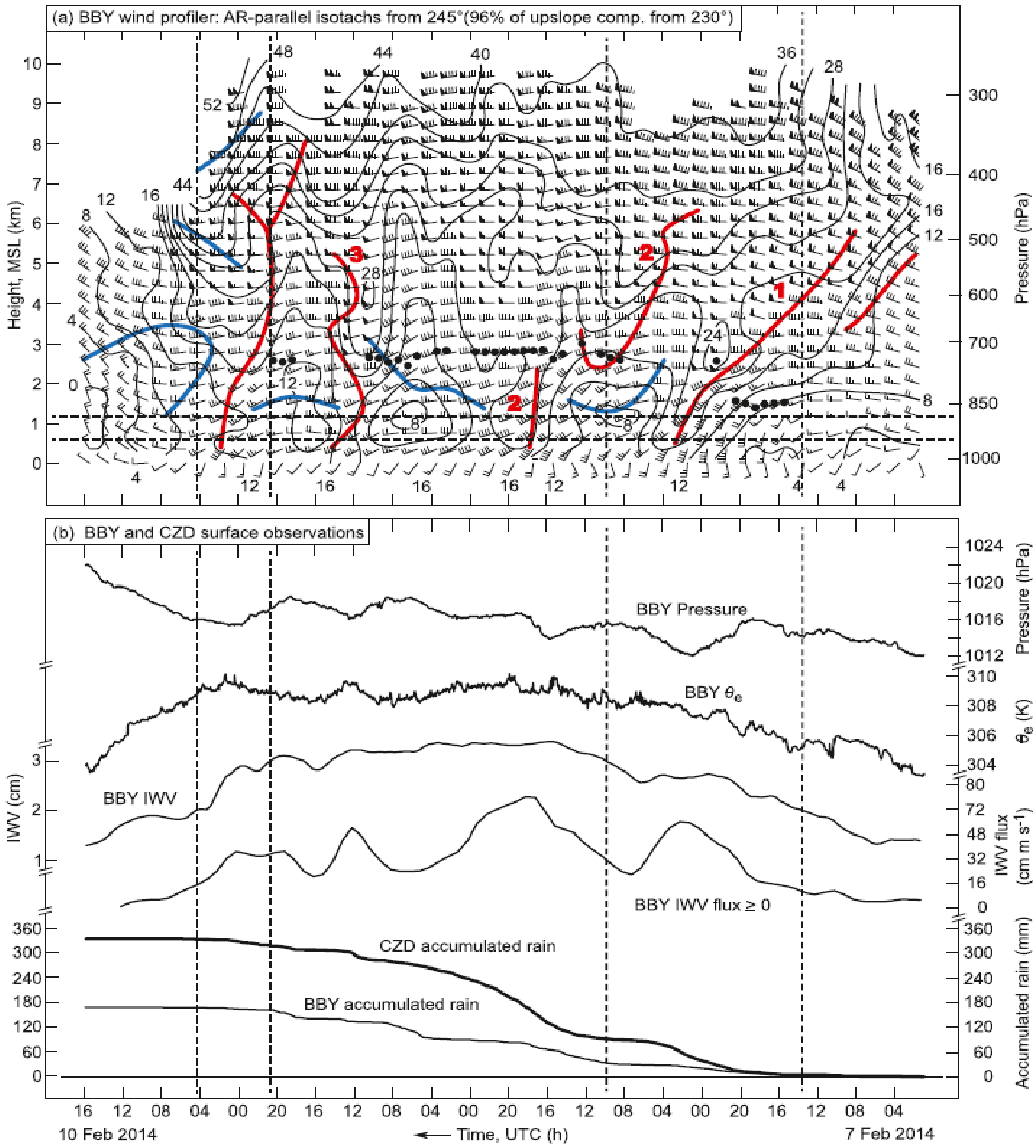

Figure.9.6 (a) Time–height section from the BBY wind profiler of hourly averaged wind profiles (flags and barbs are as in Fig. 5), ARparallel isotachs (black contours, ms^{-1}, directed from 245^{o}; 96% of the upslope component from 230^{o}), brightband melting-level heights (bold black dots), and axes of notable thermal wind-derived (i.e., geostrophic) warm and cold advection (red and blue lines, respectively), between 0100 UTC 7 Feb and 1600 UTC 10 Feb 2014. The red numbers mark the three frontal waves described in the text. The pair of horizontal dashed lines mark the vertical bounds of the upslope (i.e., AR-dominated) orographic controlling layer between 0.6 and 1.1 km MSL. Every wind profile and every other range gate is plotted. (b) Companion time series from BBY of surface pressure (hPa), surface Θe (K), IWV (cm), upslope IWV flux in the orographic controlling layer (cm m s^{-1}), and time series from BBY and CZD of accumulated rainfall (mm). The vertical thin (thick) dotted lines in both panels mark the outer temporal bounds of IWV .2 (.3) cm. Time increases from right to left to portray the advection of transient synoptic features from west to east.

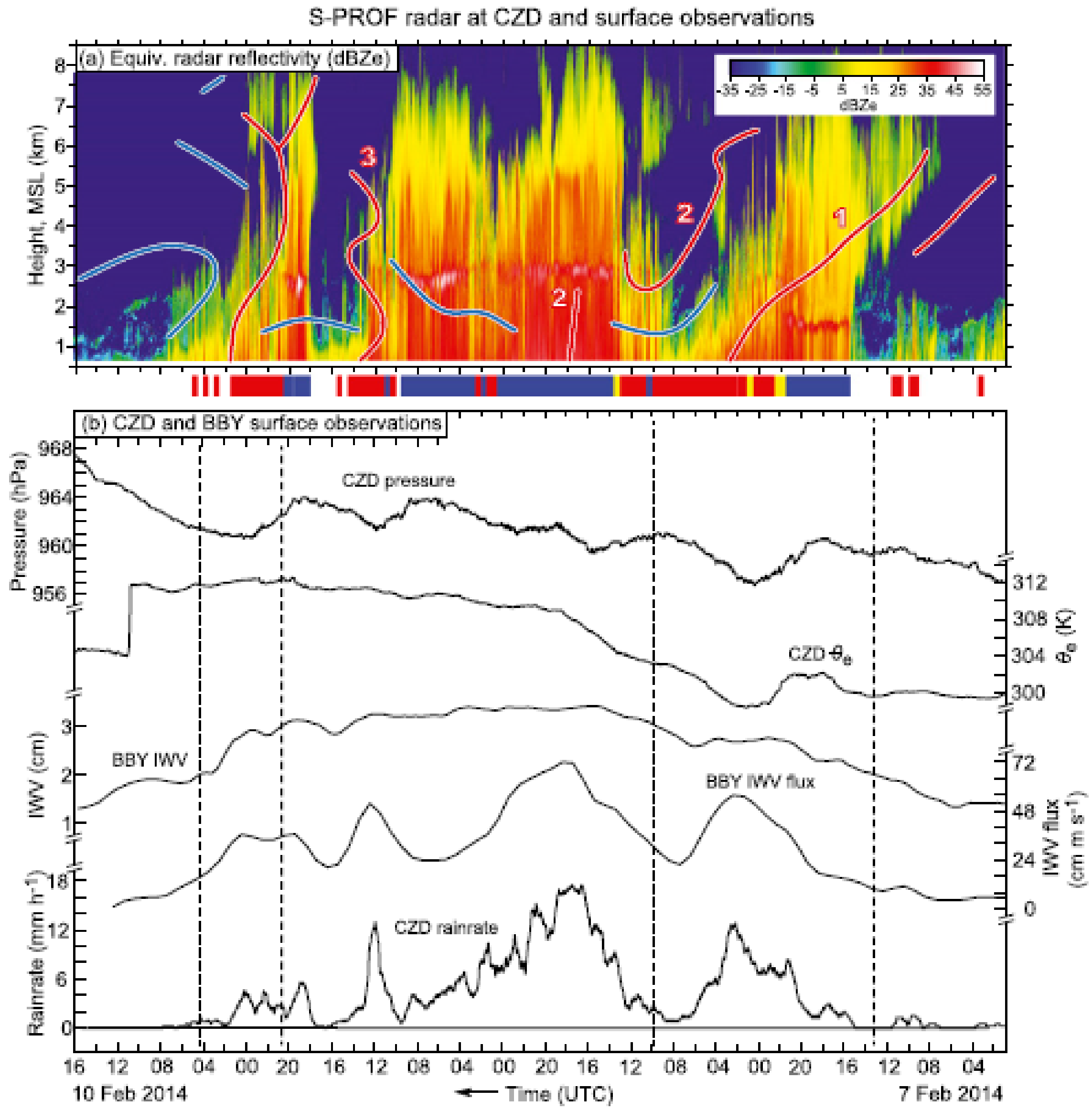

Figure 9.7 (a) Time–height section of equivalent radar reflectivity factor (dBZe) from the CZD S-PROF radar between 0100 UTC 7 Feb and 1600 UTC 10 Feb 2014. The red and blue lines (i.e., axes of geostrophic warm and cold advection at the BBY wind profiler) are as in Fig. 9.5. The red-outlined numbers mark the three frontal waves described in the text. The colored bars below represent the 30-min rainfall-type designations (blue: BB rain; red: NBB rain; yellow: convection) from the rainfall process partitioning algorithm. (b) Companion time series from CZD of surface pressure (hPa), surface u_e (K), and rain rate (mm h_{21}), and time series from BBY of IWV (cm) and upslope IWV flux in the orographic controlling layer (cmms_{21}) (as in Fig. 9.5b). The vertical thin (thick) dotted lines mark the outer temporal bounds of IWV .2 (.3) cm. Time increases from right to left to portray the advection of transient synoptic features from west to east.

10.3 Conclusions

The December and February 2014 events illustrate the effect that MFWs can have on orographic precipitation and thus forecast skill. Efforts to better understand the life cycle of MFWs on ARs are underway. The goal is to better define how the MFWs affect AR duration and location of heaviest precipitation. Research efforts include a plan for targeted observations during the upcoming field season as was done during the February 2014 event, and using analysis of AR events with and without MFWs to identify relevant signals at AROs and in synoptic scale weather patterns. Preliminary results show significant differences in low level wind direction causing differences in upslope water vapor flux values at the hourly scale, as well as differences in synoptic circulations and the location and strength of the jet stream.

Neiman, P.J., B.J. Moore, A.B. White, G.A. Wick, J. Aikins, D.L. Jackson, J.R. Spackman, F.M. Ralph,2016: An airborne and ground-based study of long-lived and intense atmospheric rivers and mesoscale frontal waves impacting California during CalWater-2014. *Mon. Wea. Rev.*,**144** ,1115-1143**.**